

The Normalised Wigner Negativity Rate as a Second-Moment Probe of Infall in AdS_3

Ritam Basu

*Department of Theoretical Physics,
Tata Institute of Fundamental Research,
1 Homi Bhabha Road, Mumbai 400005, India*

E-mail: ritam.basu@theory.tifr.res.in

ABSTRACT: In spread complexity, the average position of an operator along its Krylov chain, recovers the right radial momentum of an infalling particle in AdS, yet it is a measure of the first moment, irrespective of the spread of the wavepacket away from its classical trajectory. The rate of a normalized Krylov-Wigner negativity can be proposed as a diagnostic of the second moment of the boundary state that captures this spreading. Starting with the *seed-normalized* Krylov-Wigner distribution—that is, the Wigner transform of the descendant cloud, with the decaying return amplitude divided out—we obtain an analytic Bessel form in the macroscopic limit and compute its total negativity explicitly. Retaining the Bessel variable all the way through, we find that the negativity goes as $\sinh^{4\Delta}(\pi t/\beta)$, while the raw, seed-normalized state negativity saturates, as dictated by the $O(\sqrt{D})$ bound. Using the exact negative binomial statistics of the Krylov chain and the momentum dictionary of Caputa et al. [20], the rate of the negativity scales as the growth rate of the Krylov variance at late time asymptotics *if and only if* $\Delta = 1$, the Breitenlohner-Freedman saturating dimension in AdS_3 . This dimensionality is special in that the negativity rate is the product of the proper radial position and momentum, $\mathcal{R} \propto \mathcal{C} P_\rho$, i.e., the rate of the tidal stretch of nearby geodesic falling into the horizon. We comment on the direction for future research, in particular the interpretation of the transverse string size operator in terms of the Krylov number operator through the common $\text{SU}(1, 1)$ discrete series.

Contents

1	Introduction	2
2	Operator Growth, Spread Complexity, and the $SU(1,1)$ Algebra	3
2.1	The Lanczos Algorithm and Spread Complexity	3
2.2	Local Operator Quenches in 2D CFTs	4
2.3	The $SU(1,1)$ Algebra of the Krylov Chain	4
2.4	The Proper Momentum Correspondence	7
3	Coherent-State Amplitudes and the Seed-Normalized Distribution	7
3.1	The $SU(1,1)$ Coherent State Ansatz	7
3.2	Exact Determination of the Squeezing Parameter	9
3.3	Seed-Normalized (Return-Normalized) Amplitudes	10
3.4	Bessel Function Form of the Seed-Normalized Distribution	12
4	Normalized Negativity and Its Rate	13
4.1	Negativity of the Seed-Normalized Distribution	13
4.2	The Rate via a Real Replica Functional	13
4.3	Phase-Space Integration	14
4.4	Growth of the Normalized Negativity and Saturation of the Raw Negativity	15
5	Matching and the Critical Dimension	17
6	Negativity Rate as Tidal Momentum	20
7	Discussion	23
7.1	Summary of Boundary Results	23
7.2	Outlook	23
7.3	Future Direction: A Bulk String Interpretation	24
A	Stirling Asymptotics and the Gamma Kernel	27
B	Euler–Maclaurin Continuum Limit	28
C	Direct Evaluation of the Normalized Negativity	28
D	A Dynamical Heuristic for the Operator Identification	29

1 Introduction

The question of decoding the emergence of classical gravity and geometry from quantum dynamics of boundary conformal field theory (CFT) has been a longstanding problem of gauge-gravity duality [1–3]. Having noticed that the entanglement entropy is not a suitable characterization of late time geometry behind a black hole horizon, it was conjectured that the growing length of the Einstein-Rosen bridge is dual to the quantum complexity growth of the state on the boundary [4–9].

In contrast to the circuit complexity [10–13], which is a function of the chosen gate and reference state, the spread (or Krylov) complexity [14–19] is an intrinsic measure of operator growth. It has been found that a precise dictionary holds in the semiclassical limit between the rate of growth of the spread complexity and the proper radial momentum of an infalling particle in an AdS black hole [20].

Nevertheless, the point particle dictionary accounts only for the classical centre of mass dynamics. A wavepacket falling into a black hole is never described by a geodesic due to quantum and gravitational effects — it will necessarily *spread*. As a result, the spread complexity, the first moment of the Krylov chain (the average position along the chain), captures the motion of this centre of mass but fails to detect higher moments of the probability distribution.

Alongside other information-theoretic probes of bulk geometry [21], we suggest that the normalized generation rate of Krylov–Wigner negativity is a useful boundary observable sensitive to such spreading. The Wigner negativity is a measure of “magic” content of the Krylov phase space [23–26]; the growth of the negativity probes the holographic dictionary via the *second* moment, beyond the classical trajectory. One important structural element of our construction is the recognition that the physically meaningful object is not the raw negativity of the evolving state (normalized or not)—since it saturates when the state becomes delocalized—but a *normalized* or rescaled negativity where one divides out the trivial decay of the return amplitude. The normalized negativity and the corresponding rate are defined in section 3.

The key results in this paper are as follows. The boundary-bound negativity rate results (i)–(iii) are analytical and do not rely on any bulk conjecture:

- The seed-normalized Krylov-Wigner distribution, which is the Wigner transform of the descendant cloud with the return amplitude divided out, and the exact Bessel form expression for this distribution in the macroscopic limit ($Q \gg 1$), derived from the $SU(1, 1)$ coherent-state structure, Stirling asymptotics and the Euler-Maclaurin summation formula (see Section 3);
- The direct evaluation of the negativity of this distribution, in the entire range of the Bessel variable $Z = Q\tilde{\theta}$. The normalized negativity behaves as $\sinh^{4\Delta}(\pi t/\beta)$, whereas the raw, normalized-state negativity reaches saturation point (as dictated by its upper bound $\mathcal{N} \leq \sqrt{D}$). We find the corresponding negativity rate (Section 4);

- We demonstrate that the normalized negativity rate matches the growth rate of the variance of the Krylov wavepacket in the late-time regime *if and only if* $\Delta = 1$, the Breitenlohner-Freedman saturation dimension in AdS₃, and that at this dimension the rate is the product of proper radial position and momentum, $\mathcal{R} \propto \mathcal{C}P_\rho$, the rate of tidal stretching of neighboring infalling geodesics (Sections 5–6);
- As a direction for *future work*, we provide a possible bulk string interpretation (Section 7): Quantizing the fundamental string in AdS₃, we show that the transverse string size operator and the boundary Krylov chain possess the same quadratic Casimir $\Delta(\Delta - 1)$ and the discrete series representation D_Δ^+ of SU(1, 1) and make on this basis an operator identification conjecture $\hat{N}_{\text{str}} \simeq \hat{N}_{\text{Krylov}}$, deriving a variance map to the fluctuations of the transverse string area. We stress that this bulk reading is speculative and separate from the boundary results above.

2 Operator Growth, Spread Complexity, and the SU(1, 1) Algebra

2.1 The Lanczos Algorithm and Spread Complexity

Let us consider a Hamiltonian H that describes a chaotic holographic CFT. Heisenberg dynamics applied to a primitive local operator \mathcal{O} will generate nested commutators and thus give rise to an increasing number of non-local operators, which is usually an indicator of scrambling [28–30].

This construction can be systematically generated through the Lanczos algorithm [31], which gives rise to the basis of the Krylov subspace $\{|K_n\rangle\}_{n=0}^\infty$. The starting point is the normalized vector $|K_0\rangle = \mathcal{O}|0\rangle/\|\mathcal{O}|0\rangle\|$, and all subsequent vectors can be generated recursively according to the formula

$$|A_n\rangle = (H - a_{n-1})|K_{n-1}\rangle - b_{n-1}|K_{n-2}\rangle. \quad (2.1)$$

where the Lanczos parameters a_n and b_n are defined by

$$a_n = \langle K_n|H|K_n\rangle, \quad b_n = \|A_n\|, \quad |K_n\rangle = b_n^{-1}|A_n\rangle. \quad (2.2)$$

The matrix H is precisely *tridiagonal* relative to the orthonormal basis $\{|K_n\rangle\}$.

Spread Complexity

Expanding the time-evolved state via the conventional phase convention [14]

$$|\psi(t)\rangle = e^{-iHt}|K_0\rangle = \sum_{n=0}^{\infty} i^{-n}\psi_n(t)|K_n\rangle, \quad (2.3)$$

projecting the Schrödinger equation $\partial_t|\psi\rangle = -iH|\psi\rangle$ onto each $|K_m\rangle$ yields the single-particle hopping equation

$$\partial_t\psi_n = -i a_n\psi_n + b_n\psi_{n-1} - b_{n+1}\psi_{n+1}, \quad (2.4)$$

subject to $\psi_n(0) = \delta_{n,0}$ and $b_0 = \psi_{-1} \equiv 0$. The *spread complexity* is the mean position on this semi-infinite chain:

$$\mathcal{C}(t) = \sum_{n=0}^{\infty} n |\psi_n(t)|^2 = \langle \hat{N}_{\text{Krylov}} \rangle, \quad \hat{N}_{\text{Krylov}} = \sum_{n=0}^{\infty} n |K_n\rangle \langle K_n|. \quad (2.5)$$

2.2 Local Operator Quenches in 2D CFTs

Our focus will be on specializing to an operator \mathcal{O} of holomorphic conformal dimension Δ inserted at the origin of a 2D CFT at inverse temperature β and regulated by $\varepsilon > 0$:

$$|\psi(t)\rangle = \mathcal{N} e^{-iHt} e^{-\varepsilon H} \mathcal{O}(0) |\psi_\beta\rangle. \quad (2.6)$$

It can be shown that the above system corresponds to a planar BTZ black hole [32, 33]. In this case, the Lanczos coefficients for the moments of the return amplitude [14, 18, 34–36] take the exact closed forms

$$a_n = \frac{2\pi(n + \Delta)}{\beta \tan\left(\frac{2\pi\varepsilon}{\beta}\right)}, \quad b_n = \frac{\pi\sqrt{n(n + 2\Delta - 1)}}{\beta \sin\left(\frac{2\pi\varepsilon}{\beta}\right)}. \quad (2.7)$$

The key structural feature is $b_n^2 \propto n(n + 2\Delta - 1)$, which grows quadratically in n —the signature of the $\text{SU}(1, 1)$ discrete series algebra.

2.3 The $\text{SU}(1, 1)$ Algebra of the Krylov Chain

But these closed-form expressions (2.7) are not merely convenient for computational purposes, because the quadratic growth $b_n^2 \propto n(n + 2\Delta - 1)$ characterizes an underlying non-compact symmetry. Namely, a semi-infinite hopping chain whose off-diagonal entries grow like n as $n \rightarrow \infty$ can never be organized by a compact, finite dimensional symmetry. Instead, it is precisely the simplest realization of a lowest-weight $\mathfrak{su}(1, 1)$ module, where $\mathfrak{su}(1, 1)$ is the Lie algebra of $\text{SU}(1, 1) \cong \text{SL}(2, \mathbb{R})$ [14, 18, 36, 39]. The appearance of this symmetry is tied to the conformal structure of the problem, since the local quench (2.6) involves the primary field of dimension Δ and all its global descendants, and the global piece of the two-dimensional conformal symmetry acting only on one chiral tower is indeed $\mathfrak{su}(1, 1)$. Exposing the symmetry structure is what makes the Krylov dynamics exactly solvable, and — as we will use in section 7.3 — provides us with a framework in which to compare the boundary hopping chain and the bulk string Hilbert space.

More precisely, we introduce the generators associated with the Lie algebra $\mathfrak{su}(1, 1)$ on our chain, with the position being promoted to a Cartan generator, and ladder operators implementing the hopping dynamics. The diagonal generator $K_0^{(K)}$ keeps track of our position in the Krylov subspace (shift by Δ), while the ladder generators $K_\pm^{(K)}$ act to increase and decrease the Krylov level n . Precise matrix elements are fixed by demanding that the algebra close and that the lowering operator reproduce the Lanczos sequence (2.7).

Lemma 2.1 (SU(1, 1) structure of the thermal Krylov chain). *Define operators on $\mathcal{H}_{\text{Krylov}} = \text{span}\{|K_n\rangle\}$:*

$$K_0^{(K)} = \sum_{n=0}^{\infty} (n + \Delta) |K_n\rangle\langle K_n|, \quad (2.8)$$

$$K_+^{(K)} = \sum_{n=0}^{\infty} \sqrt{(n+1)(n+2\Delta)} |K_{n+1}\rangle\langle K_n|, \quad (2.9)$$

$$K_-^{(K)} = (K_+^{(K)})^\dagger = \sum_{n=1}^{\infty} \sqrt{n(n+2\Delta-1)} |K_{n-1}\rangle\langle K_n|. \quad (2.10)$$

These operators:

1. *satisfy the $\mathfrak{su}(1, 1)$ commutation relations*

$$[K_0^{(K)}, K_\pm^{(K)}] = \pm K_\pm^{(K)}, \quad [K_-^{(K)}, K_+^{(K)}] = 2K_0^{(K)}; \quad (2.11)$$

2. *realize the discrete series UIR D_Δ^+ of SU(1, 1) with Bargmann index $k = \Delta$ and lowest-weight state satisfying $K_-^{(K)}|K_0\rangle = 0$;*

3. *possess the quadratic Casimir*

$$C_2^{(K)} = K_0^{(K)}(K_0^{(K)} - 1) - K_+^{(K)}K_-^{(K)} = \Delta(\Delta - 1) \mathbf{1} \quad (2.12)$$

on every basis vector $|K_n\rangle$; and

4. *reproduce the Lanczos coefficients (2.7) via $b_n = \frac{\pi}{\beta \sin(2\pi\varepsilon/\beta)} \sqrt{n(n+2\Delta-1)}$.*

The four statements have distinct physical content. Item (1) certifies that $\{K_0^{(K)}, K_\pm^{(K)}\}$ genuinely generate $\mathfrak{su}(1, 1)$ and not merely a deformation of it. Item (2) identifies which representation is at play: the seed operator $|K_0\rangle$ is the lowest-weight vector, annihilated by $K_-^{(K)}$, so the Krylov chain is the orbit $\{(K_+^{(K)})^n|K_0\rangle\}$ swept out by the raising operator, and the representation is the positive discrete series D_Δ^+ labelled by the single number $k = \Delta$. Item (3) is the invariant statement underlying everything that follows—the Casimir is a c-number, fixed entirely by Δ —while item (4) confirms that this abstract structure reproduces the microscopically computed Lanczos data, so no assumption beyond the CFT two-point function has been smuggled in.

Proof. (1) Commutation relations. Acting on a generic basis vector and using (2.8)–(2.10),

$$K_0^{(K)}K_+^{(K)}|K_n\rangle = (n+1+\Delta)\sqrt{(n+1)(n+2\Delta)}|K_{n+1}\rangle, \quad (2.13)$$

$$K_+^{(K)}K_0^{(K)}|K_n\rangle = (n+\Delta)\sqrt{(n+1)(n+2\Delta)}|K_{n+1}\rangle, \quad (2.14)$$

whose difference is $[K_0^{(K)}, K_+^{(K)}]|K_n\rangle = K_+^{(K)}|K_n\rangle$, and likewise $[K_0^{(K)}, K_-^{(K)}] = -K_-^{(K)}$ by Hermitian conjugation. For the remaining relation,

$$K_-^{(K)} K_+^{(K)} |K_n\rangle = (n+1)(n+2\Delta) |K_n\rangle, \quad (2.15)$$

$$K_+^{(K)} K_-^{(K)} |K_n\rangle = n(n+2\Delta-1) |K_n\rangle, \quad (2.16)$$

so that $[K_-^{(K)}, K_+^{(K)}]|K_n\rangle = (2n+2\Delta)|K_n\rangle = 2K_0^{(K)}|K_n\rangle$, which is (2.11).

(2) *Discrete series.* The lowering operator (2.10) starts its sum at $n=1$, so its action on the seed vanishes, $K_-^{(K)}|K_0\rangle = 0$: the chain has a bottom rung and no states of negative level, the defining property of a lowest-weight module. From (2.8) the spectrum of $K_0^{(K)}$ is $\{\Delta, \Delta+1, \Delta+2, \dots\}$, equally spaced and bounded below by Δ , which is exactly the weight content of the positive discrete series D_Δ^+ with Bargmann index $k = \Delta$ [39]. The index is therefore not a free label but is pinned to the conformal dimension of the quenching operator.

(3) *Casimir.* Using $K_+^{(K)} K_-^{(K)} |K_n\rangle = n(n+2\Delta-1) |K_n\rangle$ from above,

$$\begin{aligned} C_2^{(K)} |K_n\rangle &= [(n+\Delta)(n+\Delta-1) - n(n+2\Delta-1)] |K_n\rangle \\ &= [n^2 + n(2\Delta-1) + \Delta(\Delta-1) - n^2 - n(2\Delta-1)] |K_n\rangle = \Delta(\Delta-1) |K_n\rangle. \end{aligned} \quad (2.17)$$

The level-dependent pieces n^2 and $n(2\Delta-1)$ cancel identically, so $C_2^{(K)}$ takes the same value $\Delta(\Delta-1)$ on every rung of the chain, establishing the operator identity (2.12). By Schur's lemma this constancy is the statement that the entire chain lies in a single irreducible representation.

(4) *Lanczos data.* The lower-diagonal matrix elements of $K_-^{(K)}$ in (2.10) are $\sqrt{n(n+2\Delta-1)}$, which differ from the Lanczos coefficients (2.7) only by the overall constant $\pi/[\beta \sin(2\pi\varepsilon/\beta)]$; this fixes the normalisation quoted in item (4) and matches the microscopic data exactly. \square

The most important consequence is item (3): because the Casimir is a pure number $\Delta(\Delta-1)\mathbf{1}$, the Krylov chain carries a *single* irreducible representation, characterised by Δ alone and by nothing else about the microscopic Hamiltonian. This invariant labelling is what makes a meaningful comparison with the bulk possible: any other Hilbert space that realises D_Δ^+ with the same Bargmann index shares the same Casimir, a necessary condition we return to in section 7.3.

Within this representation, the natural observable is the Cartan generator itself. The spread complexity (2.5) is the mean chain position, and comparing (2.8) with (2.5) identifies it with the shifted Cartan operator,

$$\hat{N}_{\text{Krylov}} = K_0^{(K)} - \Delta \cdot \mathbf{1}, \quad (2.18)$$

so that \hat{N}_{Krylov} has spectrum $\{0, 1, 2, \dots\}$ and counts levels above the lowest-weight seed. Finally, the tridiagonal Krylov Hamiltonian—diagonal part a_n plus hopping b_n from (2.7)—is, in view of (2.8)–(2.10), a real linear combination of $K_0^{(K)}$ and $K_\pm^{(K)}$, i.e. an element of

$\mathfrak{su}(1, 1)$. Consequently the evolution operator e^{-iHt} is a group element, and acting on the lowest-weight state it produces an $SU(1, 1)$ (Perelomov) coherent state. This is the structural reason the occupation amplitudes assemble into the closed coherent-state form of section 3.1, and ultimately into the negative-binomial distribution of Lemma 3.1.

2.4 The Proper Momentum Correspondence

The $SU(1, 1)$ symmetry in the semiclassical regime of large- n is used by Caputa et al. [20] to establish the result that the speed of spread complexity matches the proper radial momentum of an infalling massive point particle within the BTZ background:

$$\frac{d\mathcal{C}}{dt} \propto P_\rho(t). \quad (2.19)$$

This classical equivalence holds only for the *first moment* $\langle \hat{N}_{\text{Krylov}} \rangle$. However, to study how the width of the wavefunction distribution changes—or how the state departs from the point-particle approximation—requires access to higher moments and hence the full Wigner phase-space geometry.

3 Coherent-State Amplitudes and the Seed-Normalized Distribution

3.1 The $SU(1, 1)$ Coherent State Ansatz

The algebraic structure found in section 2.3 largely determines the evolved state. The tridiagonal Krylov Hamiltonian being an element of $\mathfrak{su}(1, 1)$, the evolution operator e^{-iHt} is a group element, and it acts on the lowest-weight seed $|K_0\rangle$ to generate an $SU(1, 1)$ (Perelomov) coherent state [14, 18, 39]—the group-theoretic analog of a squeezed vacuum. Such states are characterised by a single complex number, the squeezing parameter $A(t)$, whose square determines the wavefunction of the coherent state on the n -th rung of the chain through the representation D_Δ^+ ,

$$\psi_n(t) = \sqrt{\frac{\Gamma(2\Delta + n)}{n! \Gamma(2\Delta)}} A(t)^n \psi_0(t). \quad (3.1)$$

The combinatorial prefactor is the norm of the state $(K_+^{(K)})^n |K_0\rangle$ in the representation D_Δ^+ , so (3.1) is not an approximation but the exact wavefunction of a coherent state on the chain, with a single unknown $A(t)$ determined from the dynamics in section 3.2. Normalising the probability current through $\sum_n |\psi_n(t)|^2 = 1$ and evaluating the geometric-type series fixes the seed amplitude,

$$|\psi_0(t)|^2 = (1 - |A(t)|^2)^{2\Delta}, \quad (3.2)$$

which is real and positive precisely if $|A(t)| < 1$, corresponding to the physically sensible regime of a normalisable coherent state.

From (3.1) follows an immediate consequence for the statistics: the probabilities $p_n(t) = |\psi_n(t)|^2$ are not any old sequence, but they constitute a *one-parameter family*, controlled by $|A(t)|^2$ alone. This one-parameter family turns out to be a well-known distribution—the

negative binomial—which we now introduce in a closed form, since its moments will become the boundary values for the bulk string geometry.

Lemma 3.1 (Negative Binomial Distribution). *The probability distribution given by (3.1) is the NB($2\Delta, |A(t)|^2$):*

$$|\psi_n(t)|^2 = \binom{n + 2\Delta - 1}{n} |A(t)|^{2n} (1 - |A(t)|^2)^{2\Delta}, \quad (3.3)$$

with exact mean and variance

$$\langle \hat{N}_{\text{Krylov}} \rangle = \frac{2\Delta |A(t)|^2}{1 - |A(t)|^2}, \quad (3.4)$$

$$\text{Var}(\hat{N}_{\text{Krylov}}) = \frac{2\Delta |A(t)|^2}{(1 - |A(t)|^2)^2}. \quad (3.5)$$

The two parameters have an evident interpretation. The number of “failures”, $r = 2\Delta$, equals twice the Bargmann index of the representation, so the dimension of the quenching operator controls directly the shape of the distribution. The “success probability”, $p = |A(t)|^2$, is the measure of squeezing, monotonously increasing towards unity as the state spreads down the chain. As $|A| \rightarrow 1$, both moments diverge, indicating the spreading of the wavepacket characteristic of operator growth in a chaotic theory. (On a true finite-dimensional chain the spreading is capped by the Heisenberg time, after which the Krylov-Wigner negativity plateaus [23]. The coherent-state description below works up to the plateau, in the macroscopic regime.)

Proof. Substituting (3.1) and the normalisation (3.2), the probability of the level- n is

$$|\psi_n|^2 = (1 - |A|^2)^{2\Delta} \frac{\Gamma(2\Delta + n)}{n! \Gamma(2\Delta)} |A|^{2n} = \binom{n + 2\Delta - 1}{n} (1 - |A|^2)^{2\Delta} |A|^{2n},$$

where the second equality used $\Gamma(2\Delta + n)/[n! \Gamma(2\Delta)] = \binom{n + 2\Delta - 1}{n}$. This is precisely the negative binomial distribution NB($2\Delta, |A|^2$) with $r = 2\Delta$ and $p = |A|^2$. Its first two moments are given by the generating function $G(z) = \sum_n p_n z^n = (1 - p)^r (1 - pz)^{-r}$: differentiating at $z = 1$ yields the mean $G'(1) = rp/(1 - p)$, which is (3.4), and the variance $G''(1) + G'(1) - [G'(1)]^2 = rp/(1 - p)^2$, which is (3.5). \square

There are two features of Lemma 3.1 which drive the analysis of the paper. First, comparing the two moments demonstrates that the distribution is *overdispersed*, i.e. the variance contains an extra factor of $(1 - |A|^2)^{-1}$ compared to the mean, and thus grows faster as the state delocalises. Expressing this relation in terms of the squeezing parameter leads to the exact identity

$$\text{Var}(\hat{N}_{\text{Krylov}}) = \langle \hat{N}_{\text{Krylov}} \rangle + \frac{1}{2\Delta} \langle \hat{N}_{\text{Krylov}} \rangle^2, \quad (3.6)$$

which we use in section 7 to identify the bulk geometry of the boundary statistics. Second, since the whole distribution depends on the single combination $|A(t)|^2$, the time dependence of any moment can be expressed in terms of $|A(t)|^2$ alone; once $A(t)$ is determined in section 3.2, the late-time scalings $\langle \hat{N}_{\text{Krylov}} \rangle \sim \sinh^2(\pi t/\beta)$ and $\text{Var}(\hat{N}_{\text{Krylov}}) \sim \sinh^4(\pi t/\beta)$ follow.

3.2 Exact Determination of the Squeezing Parameter

The coherent-state ansatz (3.1) reduces the entire evolved state to a single unknown function—the squeezing parameter $A(t)$. We now fix it from the dynamics. Naively, this would involve solving the complete infinite hopping problem of (2.4). But the $\text{SU}(1,1)$ structure of section 2.3 implies that the coherent state remains coherent under the group evolution. So the evolution equation must be solved by just a *single* component: the rest of the components are automatically satisfied by the algebra. The easiest component to work with is the lowest component of the Schrödinger equation. Setting $n = 0$ in (2.4), where $b_0 = 0$ and $\psi_{-1} \equiv 0$ truncate the recursion, and using the expression for ψ_1 from (3.1), we obtain a first-order differential equation for the seed amplitude alone,

$$\partial_t \psi_0 = -i a_0 \psi_0 - b_1 \sqrt{2\Delta} A \psi_0. \quad (3.7)$$

Dividing this equation through by ψ_0 eliminates the need for the global normalisation and exposes A explicitly:

$$\boxed{A(t) = \frac{-\partial_t \ln \psi_0(t) - i a_0}{b_1 \sqrt{2\Delta}}}. \quad (3.8)$$

Therefore, $A(t)$ is uniquely determined by knowing a single function $\psi_0(t)$.

This function is not arbitrary: $\psi_0(t) = \langle K_0 | \psi(t) \rangle$ is the return amplitude of the quench, and for a primary operator \mathcal{O} of the dimension Δ in a 2D thermal CFT the amplitude is fixed by conformal invariance to be the regularised thermal two-point function,

$$\psi_0(t) = \left[\frac{\sinh\left(\frac{\pi(t-2i\varepsilon)}{\beta}\right)}{\sinh\left(\frac{-2\pi i\varepsilon}{\beta}\right)} \right]^{-2\Delta}, \quad (3.9)$$

where ε is the Euclidean smearing of the operator—a regularization that makes the inserted operator normalisable and provides the standard $t \rightarrow t - 2i\varepsilon$ prescription. Its logarithmic time derivative is elementary,

$$\partial_t \ln \psi_0(t) = -\frac{2\pi\Delta}{\beta} \coth\left(\frac{\pi(t-2i\varepsilon)}{\beta}\right). \quad (3.10)$$

Substituting a_0 and $b_1 \sqrt{2\Delta}$ from the Lanczos data (2.7) and the above $\partial_t \ln \psi_0$ into (3.8), the common factor $2\pi\Delta/\beta$ cancels, yielding the intermediate expression

$$A(t) = \frac{\coth\left(\frac{\pi(t-2i\varepsilon)}{\beta}\right) - i \cot\left(\frac{2\pi\varepsilon}{\beta}\right)}{\csc\left(\frac{2\pi\varepsilon}{\beta}\right)}. \quad (3.11)$$

This cancellation is important: it shows that $A(t)$ does not depend on Δ . The conformal dimension Δ does not enter into the expression for the squeezing parameter at all, it only enters as the parameter $r = 2\Delta$ of the occupation statistics of Lemma 3.1. Consequently the time dependence of the *shape* of the Krylov wavepacket (and thus the functional form of every scaling derived below) becomes universal, while Δ only dictates the relative weight. This universality allows to derive a single matching condition that chooses the critical dimension in section 5.

The remaining manipulation is simple trigonometry: setting $a = \pi t/\beta$ and $b = 2\pi\varepsilon/\beta$ and combining (3.11) over the common denominator $\sin(b)[\sinh^2(a) + \sin^2(b)]$, the numerator of $\coth(a - ib) - i \cot(b)$ simplifies to $\sinh(a)[\cosh(a) \sin(b) - i \sinh(a) \cos(b)]$. Recognising the bracket as $-i \sinh(a + ib)$ and using $\sinh^2(a) + \sin^2(b) = |\sinh(a + ib)|^2 = \sinh(a + ib) \sinh(a - ib)$ to factor the denominator, we obtain the compact expression

$$A(t) = \frac{-i \sinh(\pi t/\beta)}{\sinh\left(\frac{\pi(t-2i\varepsilon)}{\beta}\right)}. \quad (3.12)$$

This shows that the squeezing parameter is the ratio of thermal sines: its modulus encodes the spreading of the wavepacket, while the explicit $-i$ and the regulator give the phase $\varphi_A(t)$ necessary to rotate the Wigner distribution of section 3.4.

Remark 3.2. Since $|\sinh(x \pm iy)|^2 = \sinh^2(x) + \sin^2(y)$ does not depend on the sign of y , two forms of $A(t)$ that have the same $|A(t)|^2$ yield identical physics. From (3.12) one can see that the late-time behaviour of $|A(t)|^2$ is given by $|A|^2 \rightarrow 1 - \sin^2(2\pi\varepsilon/\beta)/\sinh^2(\pi t/\beta)$.

In other words, $|A(t)|^2 = \sinh^2(\pi t/\beta)/[\sinh^2(\pi t/\beta) + \sin^2(2\pi\varepsilon/\beta)]$, such that the complementary factor $1 - |A(t)|^2$ is exactly the quantity $\xi(t)$ defined in (4.9). Substituting this into (3.4)-(3.5) gives the \sinh^2 and \sinh^4 growth rates behind the negativity and variance rate derived in the subsequent sections.

3.3 Seed-Normalized (Return-Normalized) Amplitudes

Before building the phase space distribution it is important to normalise the state, because the normalisation choice dictates which quantity carries the physical information. The evolved state on the chain, $|\psi(t)\rangle = \sum_n i^{-n} \psi_n(t) |K_n\rangle$, is always normalized, $\sum_n |\psi_n(t)|^2 = 1$. The negativity of the Wigner function of such a state, as we will see, saturates, because the quasi-probability distribution spreads out further and further over the phase space while getting smaller in height, keeping the total quasi-probability constant. That saturation is the statement about the return amplitude decaying, not the geometric spreading we wish to capture.

Introducing the *return probability*

$$\mathcal{P}(t) \equiv |\psi_0(t)|^2 = (1 - |A(t)|^2)^{2\Delta}, \quad (3.13)$$

it should be emphasized that the evolved state is always normalized for *any* t and for *any* β . By the unitarity the state $|\psi(t)\rangle = e^{-iHt} |K_0\rangle$ is always normalised, which means that the

equality (3.13) guarantees $\sum_n |\psi_n|^2 = |\psi_0|^2 \sum_n \binom{n+2\Delta-1}{n} |A|^{2n} = |\psi_0|^2 (1 - |A|^2)^{-2\Delta} = 1$ at any temperature, with no distinguished value of β where normalisation fails. Therefore the Wigner function of the state satisfies $\sum_{Q,p} W(Q,p,t) = \text{Tr } \rho = 1$ at any β . The renormalisation procedure we introduce below is *not* an operation restoring the normalisation, it is only to strip the return amplitude and to leave the geometric spreading.

To expose the spreading we therefore normalize the amplitudes right from the start. We define the *seed-normalized* (return-normalized) amplitudes

$$\chi_n(t) \equiv \frac{\psi_n(t)}{\psi_0(t)} = \sqrt{\frac{\Gamma(2\Delta + n)}{n! \Gamma(2\Delta)}} A(t)^n, \quad \chi_0(t) = 1. \quad (3.14)$$

These are the amplitudes of the descendant cloud *relative to the surviving seed*. The overall phase and magnitude of the return amplitude have been stripped off, leaving the form of the spreading packet. Their norm square sums up to the inverse survival probability,

$$\sum_{n=0}^{\infty} |\chi_n(t)|^2 = \frac{1}{\mathcal{P}(t)} = (1 - |A(t)|^2)^{-2\Delta}, \quad (3.15)$$

that diverges when the state delocalizes ($|A| \rightarrow 1$), and serves the purpose of an effective number of visited descendants.

Consequently the *seed-normalized Krylov–Wigner distribution* is introduced as the discrete Wigner function of the χ_n ,

$$\mathcal{W}(Q,p,t) \equiv \frac{1}{D} \sum_{m=-Q}^Q e^{4\pi i m p / D} \chi_{Q+m}(t) \chi_{Q-m}^*(t) = \frac{W(Q,p,t)}{\mathcal{P}(t)}, \quad (3.16)$$

where W is the Wigner function of the normalized state. As $\sum_{Q,p} W = \text{Tr } \rho = 1$, the quasi-probability of the seed-normalized distribution is equal to (3.15),

$$\sum_{Q,p} \mathcal{W}(Q,p,t) = \frac{1}{\mathcal{P}(t)}. \quad (3.17)$$

Alternatively, \mathcal{W} is the Wigner transform of the *unnormalized* descendant operator $\rho_{\text{desc}}(t) = |\psi(t)\rangle\langle\psi(t)|/\mathcal{P}(t)$.

Remark 3.3 (What \mathcal{W} is, and is not). As a matter of construction \mathcal{W} is *not* the Wigner function of a normalized state: its quasi-probability (3.17) is $1/\mathcal{P}(t) \neq 1$. It is a rescaled phase-space quantity—the negativity computed from it below is proportional to the raw (normalized-state) negativity divided by the survival probability, i.e. the magic content per unit surviving return amplitude. The normalization procedure is not a projective post-selection onto a certain subspace; instead it is just the uniform rescaling by $1/\mathcal{P}(t)$, which compensates for the return amplitude decay. It is precisely the meaning of the “normalized negativity” in section 4. This is what makes the geometric spreading (and not probability leakage) the growing quantity. In Remark 4.4 we discuss the implications of this choice of normalization for the matching problem.

3.4 Bessel Function Form of the Seed-Normalized Distribution

We derive here the closed form of \mathcal{W} in the macroscopic regime $Q \gg 1$, in which the excitation is deeply inside the chain and the dual description holds. Since χ_n differs from ψ_n only by stripping the common factor $\psi_0(t)$, the procedure is that of finding the Wigner function of an $SU(1, 1)$ coherent state without the overall survival factor. Substituting the definition of χ_n in (3.14) to (3.16), and noting that $A(t) = |A(t)|e^{i\varphi_A}$, the resulting phases unite into one linear exponent, and the magnitude factors turn into a ratio of the Gamma functions,

$$\mathcal{W}(Q, p, t) = \frac{|A(t)|^{2Q}}{D\Gamma(2\Delta)} \sum_{m=-Q}^Q e^{im(4\pi p/D + 2\varphi_A)} \frac{\sqrt{\Gamma(2\Delta + Q + m)\Gamma(2\Delta + Q - m)}}{\sqrt{(Q + m)!(Q - m)!}}. \quad (3.18)$$

The prefactor is the pure geometric factor $|A|^{2Q}$; all the phase-space oscillations arise from the summand, where the kernel of the sum $K(Q, m)$ (the ratio of Gamma functions) sets the profile in the shift variable m , and the exponential gives the phase depending on the conjugate momentum $4\pi p/D + 2\varphi_A$.

Two standard techniques help to linearize the sum. First, by the asymptotics of Stirling (Appendix A) the kernel simplifies to a smooth power-law form,

$$K(Q, m) \approx Q^{2\Delta-1} (1 - x^2)^{\Delta-1/2}, \quad x \equiv m/Q \in [-1, 1]. \quad (3.19)$$

Second, since $\Delta > 1/2$ the profile vanishes at $x = \pm 1$; so the Euler–Maclaurin summation formula (Appendix B) converts the sum to the integral with no boundary term,

$$Q^{2\Delta} \int_{-1}^1 (1 - x^2)^{\Delta-1/2} e^{iZx} dx, \quad Z \equiv Q \left(\frac{4\pi p}{D} + 2\varphi_A \right),$$

so that the single rescaled variable Z carries the entire phase-space dependence. This integral is Poisson’s representation of the Bessel function: for any $\Delta > -\frac{1}{2}$,

$$\int_{-1}^1 (1 - x^2)^{\Delta-1/2} e^{iZx} dx = \sqrt{\pi} \Gamma\left(\Delta + \frac{1}{2}\right) \left(\frac{2}{Z}\right)^\Delta J_\Delta(Z). \quad (3.20)$$

Combining (3.20) with the prefactor of (3.18) and using Legendre duplication $\Gamma(2\Delta) = 2^{2\Delta-1} \pi^{-1/2} \Gamma(\Delta) \Gamma(\Delta + \frac{1}{2})$ to collapse the Gamma and power-of-two factors, we obtain the closed-form seed-normalized distribution at leading order in the macroscopic limit:

$$\boxed{\mathcal{W}(Q, p, t) \approx \frac{\pi |A(t)|^{2Q} Q^{2\Delta}}{D 2^{2\Delta-1} \Gamma(\Delta) Z^\Delta} J_\Delta(Z)}. \quad (3.21)$$

Equation (3.21) is a *leading macroscopic (continuum) expression*, not an exact finite-chain result. Relative to the normalised-state Wigner function it is cleaner: the survival factor $\mathcal{P}(t) = |\psi_0|^2$ is absent, having been divided out at the level of the amplitudes (3.14). The everywhere-positive envelope $|A|^{2Q} Q^{2\Delta}$ fixes the radial extent, while the oscillatory factor $J_\Delta(Z)/Z^\Delta$ —and in particular its sequence of sign-changing zeros—produces the alternating troughs of quasi-probability whose total we compute next. These negative troughs, absent for any Gaussian (classical) state, are the non-classical content diagnosing that the infalling excitation is not a structureless point particle.

4 Normalized Negativity and Its Rate

4.1 Negativity of the Seed-Normalized Distribution

The non-classicality of the descendant cloud is measured by the total negativity of the seed-normalized distribution, its phase-space 1-norm,

$$\mathcal{N}(t) \equiv \sum_{Q,p} |\mathcal{W}(Q, p, t)| = \frac{1}{\mathcal{P}(t)} \sum_{Q,p} |W(Q, p, t)| = \frac{\mathcal{N}_{\text{raw}}(t)}{\mathcal{P}(t)}, \quad (4.1)$$

where $\mathcal{N}_{\text{raw}}(t) = \sum_{Q,p} |W|$ is the negativity of the normalised state, which obeys the rigorous bound $1 \leq \mathcal{N}_{\text{raw}} \leq \sqrt{D}$ [23] and, as shown below, saturates at an $O(1)$, Δ -dependent constant within the regime of validity of the macroscopic description. Thus $\mathcal{N}(t)$ is the magic content per unit surviving return amplitude (Remark 3.3); dividing out \mathcal{P} removes the trivial decay of the return amplitude and leaves the geometric growth.

4.2 The Rate via a Real Replica Functional

Differentiating $\mathcal{N}(t)$ is delicate because $|\mathcal{W}|$ is kinked wherever \mathcal{W} vanishes, i.e. on the moving zero set of $J_\Delta(Z)$. We regulate with a smooth surrogate.

Definition 4.1 (Real Replica Functional). For $k > 1/2$, define the strictly real, non-negative functional

$$\mathcal{N}^{(k)}(t) = \sum_{Q,p} (\mathcal{W}(Q, p, t)^2)^k, \quad \lim_{k \rightarrow 1/2} \mathcal{N}^{(k)}(t) = \mathcal{N}(t). \quad (4.2)$$

For $k > 1/2$ the summand is a smooth function of \mathcal{W} , so $\mathcal{N}^{(k)}$ may be differentiated term by term; sending $k \rightarrow \frac{1}{2}$ afterwards restores $|\mathcal{W}|$.

Proposition 4.2 (Negativity rate). *The rate of the negativity is*

$$\mathcal{R}(t) \equiv \dot{\mathcal{N}}(t) = \sum_{Q,p} \text{sgn}(\mathcal{W}) \partial_t \mathcal{W} = \frac{d}{dt} \left(\frac{1}{\mathcal{P}(t)} \right) - 2 \sum_{\Omega_-} \partial_t \mathcal{W}(Q, p, t), \quad (4.3)$$

where $\Omega_- = \{(Q, p) : \mathcal{W} < 0\}$. When the distribution has conserved total weight—as does the normalised-state W , for which $\sum_{Q,p} W = 1$ —the first term is absent and the rate is the pure inward flux $\mathcal{R}_{\text{raw}} = -2 \sum_{\Omega_-} \partial_t W$.

Proof. Differentiating (4.2) term by term, $\partial_t (\mathcal{W}^2)^k = 2k(\mathcal{W}^2)^{k-1} \mathcal{W} \partial_t \mathcal{W} \rightarrow \text{sgn}(\mathcal{W}) \partial_t \mathcal{W}$ as $k \rightarrow \frac{1}{2}$ at every point with $\mathcal{W} \neq 0$; the zero set is of measure zero and $\partial_t \mathcal{W}$ is finite there. This gives the first equality. Splitting phase space into Ω_\pm where $\mathcal{W} \gtrless 0$ and writing $\sum_{\Omega_+} \partial_t \mathcal{W} = \sum_{Q,p} \partial_t \mathcal{W} - \sum_{\Omega_-} \partial_t \mathcal{W}$,

$$\mathcal{R} = \sum_{\Omega_+} \partial_t \mathcal{W} - \sum_{\Omega_-} \partial_t \mathcal{W} = \sum_{Q,p} \partial_t \mathcal{W} - 2 \sum_{\Omega_-} \partial_t \mathcal{W}.$$

Finally $\sum_{Q,p} \partial_t \mathcal{W} = \partial_t \sum_{Q,p} \mathcal{W} = \partial_t (1/\mathcal{P})$ by (3.17), which vanishes precisely when the total weight is conserved. \square

Equation (4.3) has a transparent reading: for a trace-preserving (normalised) distribution the negativity changes only by quasi-probability flowing across the zero locus into the negative cells; for the seed-normalized \mathcal{W} there is, in addition, the rescaling term $\partial_t(1/\mathcal{P})$ that accounts for the growth of the descendant weight. We now evaluate $\mathcal{N}(t)$ in closed form and obtain its rate by differentiation.

4.3 Phase-Space Integration

We evaluate (4.1) directly from the Bessel form (3.21), *retaining the Bessel variable* $Z = Q\tilde{\theta}$ throughout, with $\tilde{\theta} \equiv 4\pi p/D + 2\varphi_A$. Care is required with the discrete-to-continuum measure: three factors of two arise, each with a definite lattice origin, and we record them explicitly.

(i) The momentum sum and the mirror copy. As p runs over $\{0, 1, \dots, D-1\}$, the angle $\tilde{\theta} = 4\pi p/D + 2\varphi_A$ sweeps an interval of total length 4π —*two* full periods of the phase $e^{im\tilde{\theta}}$, because of the doubled frequency $4\pi/D$ inherited from the midpoint parametrisation $k - \ell = 2m$. The Bessel profile $|J_\Delta(Q\tilde{\theta})|/|Q\tilde{\theta}|^\Delta$ is localised about $\tilde{\theta} \equiv 0 \pmod{2\pi}$, so the momentum sum picks up *two* mirror copies of the distribution, centred at lattice momenta separated by $D/2$. (This doubling is directly visible in the exact discrete Wigner function: for a bulk row Q the two maxima of $|W(Q, p)|$ over p sit half a period apart.) Hence

$$\sum_{p=0}^{D-1} \longrightarrow \frac{D}{4\pi} \int_0^{4\pi} d\tilde{\theta} = 2 \times \frac{D}{4\pi} \int_{\text{one period}} d\tilde{\theta}. \quad (4.4)$$

(ii) The angular integral. Within one period, changing variables $Z = Q\tilde{\theta}$ ($d\tilde{\theta} = dZ/Q$) supplies an explicit $1/Q$, and the envelope is *even* in Z , decaying on both sides of the peak:

$$\int_{\text{one period}} d\tilde{\theta} \frac{|J_\Delta(Z)|}{|Z|^\Delta} = \frac{1}{Q} \int_{-\infty}^{\infty} dZ \frac{|J_\Delta(Z)|}{|Z|^\Delta} = \frac{2c_\Delta}{Q}, \quad c_\Delta \equiv \int_0^{\infty} \frac{|J_\Delta(Z)|}{Z^\Delta} dZ. \quad (4.5)$$

Here $c_\Delta < \infty$ for every $\Delta > 1/2$: the integrand is regular at $Z = 0$ ($\rightarrow 2^{-\Delta}/\Gamma(\Delta + 1)$) and decays as $Z^{-\Delta-1/2}$ at large Z . Two remarks are in order. First, the angular integral is manifestly *not* Q -independent; the large- Z (Hankel) form alone would produce a spurious divergence at $\tilde{\theta} \rightarrow 0$, exactly the region $Z \lesssim 1$ where that form is invalid and which supplies the $1/Q$. Second, this factor reduces the radial power from $Q^{2\Delta}$ to $Q^{2\Delta-1}$ —the correction responsible for the saturation derived below.

(iii) The radial sum. The midpoint coordinate $Q = \frac{1}{2}(k + \ell)$ lives on the *half-integer* lattice $\{0, \frac{1}{2}, 1, \frac{3}{2}, \dots\}$ with spacing $\frac{1}{2}$, so

$$\sum_Q \longrightarrow 2 \int_0^{\infty} dQ. \quad (4.6)$$

Assembly. Combining (4.4)–(4.6) with the Bessel form (3.21) and $|A|^{2Q} = e^{-2Q|\ln|A||}$,

$$\begin{aligned}\mathcal{N}(t) &\approx 2 \int_0^\infty dQ \left(\frac{D}{4\pi}\right) \frac{\pi Q^{2\Delta}}{D 2^{\Delta-1}\Gamma(\Delta)} e^{-2Q|\ln|A||} \times \frac{4c_\Delta}{Q} \\ &= \frac{2c_\Delta}{2^{\Delta-1}\Gamma(\Delta)} \int_0^\infty dQ Q^{2\Delta-1} e^{-2Q|\ln|A||} = \frac{2c_\Delta}{2^{\Delta-1}\Gamma(\Delta)} \frac{\Gamma(2\Delta)}{(2|\ln|A||)^{2\Delta}},\end{aligned}\quad (4.7)$$

so that

$$\boxed{\mathcal{N}(t) \approx \frac{c_\Delta \Gamma(2\Delta)}{2^{\Delta-2}\Gamma(\Delta)} \frac{1}{(2|\ln|A(t)||)^{2\Delta}} = \frac{2^{\Delta+1}}{\sqrt{\pi}} \Gamma\left(\Delta + \frac{1}{2}\right) c_\Delta \frac{1}{(2|\ln|A(t)||)^{2\Delta}},}\quad (4.8)$$

the second form following from Legendre duplication $\Gamma(2\Delta) = 2^{2\Delta-1}\pi^{-1/2}\Gamma(\Delta)\Gamma(\Delta + \frac{1}{2})$. Because the survival factor was removed at the level of the amplitudes (3.14), no cancellation occurs here and the seed-normalized negativity is a genuinely growing function of time—in contrast to the raw negativity, to which we turn below for a consistency check.

4.4 Growth of the Normalized Negativity and Saturation of the Raw Negativity

Introduce the late-time variable

$$\varepsilon_0 \equiv \sin^2\left(\frac{2\pi\varepsilon}{\beta}\right), \quad \xi(t) \equiv 1 - |A(t)|^2 = \frac{\varepsilon_0}{S^2 + \varepsilon_0}, \quad S \equiv \sinh(\pi t/\beta),\quad (4.9)$$

so that $2|\ln|A|| = -\ln(1 - \xi) \simeq \xi \simeq \varepsilon_0/S^2$ at late times. Then the seed-normalized negativity (4.8) grows as

$$\boxed{\mathcal{N}(t) \simeq \frac{c_\Delta \Gamma(2\Delta)}{2^{\Delta-2}\Gamma(\Delta)} \frac{\sinh^{4\Delta}(\pi t/\beta)}{\sin^{4\Delta}(2\pi\varepsilon/\beta)},}\quad (4.10)$$

with rate

$$\boxed{\mathcal{R}(t) \simeq \frac{c_\Delta \Gamma(2\Delta)}{2^{\Delta-2}\Gamma(\Delta)} \frac{4\Delta\pi}{\beta} \frac{\sinh^{4\Delta-1}(\pi t/\beta) \cosh(\pi t/\beta)}{\sin^{4\Delta}(2\pi\varepsilon/\beta)}.\quad (4.11)$$

Consistency with the normalised-state picture is immediate: by (4.1) the raw negativity is $\mathcal{N}_{\text{raw}}(t) = \mathcal{P}(t)\mathcal{N}(t)$, and with $\mathcal{P} = |\psi_0|^2 = \xi^{2\Delta}$,

$$\mathcal{N}_{\text{raw}}(t) = \frac{c_\Delta \Gamma(2\Delta)}{2^{\Delta-2}\Gamma(\Delta)} \left(\frac{\xi}{-\ln(1 - \xi)}\right)^{2\Delta} \xrightarrow{\xi \rightarrow 0} \frac{c_\Delta \Gamma(2\Delta)}{2^{\Delta-2}\Gamma(\Delta)},\quad (4.12)$$

so the raw, normalised-state negativity *saturates* to a constant. The growth (4.10) is therefore carried entirely by the seed normalization, exactly as intended. Note, for large Δ the saturation value of raw negativity $\mathcal{N}_{\text{raw}}(\infty)$ is 2 i.e. $\lim_{\Delta \rightarrow \infty} \mathcal{N}_\infty = 2$. Now we make the saturation statement precise.

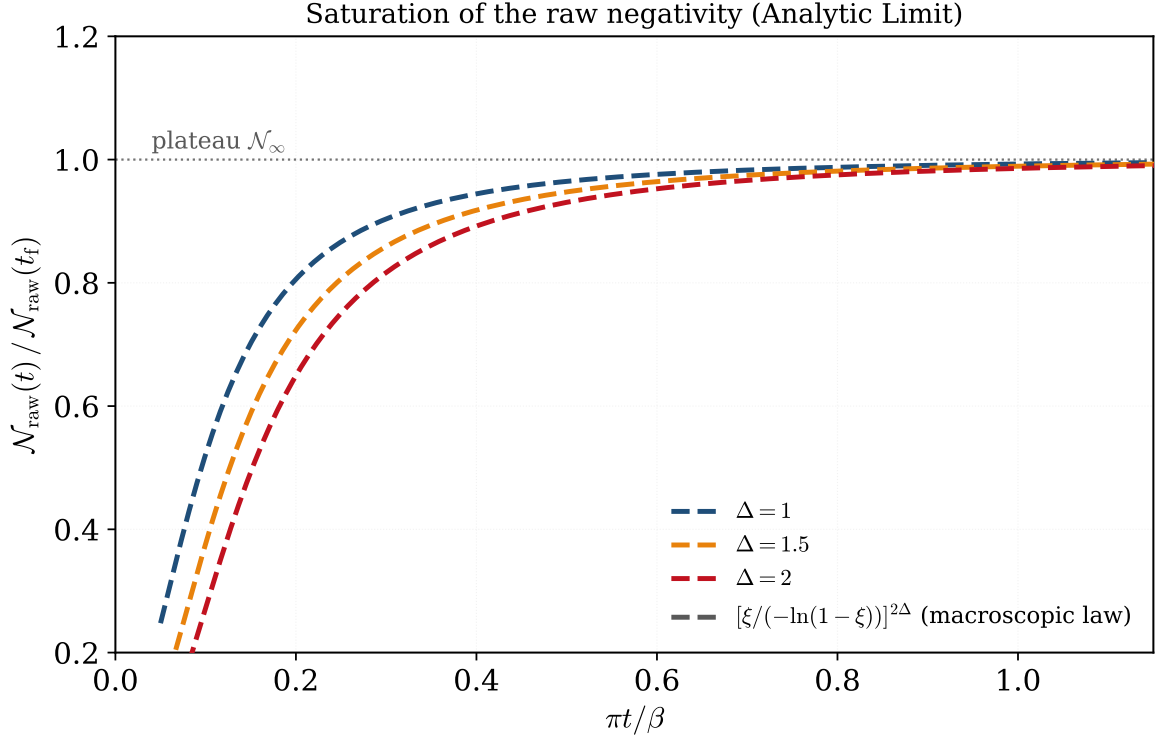


Figure 1. Saturation of the raw negativity (Analytic Limit). Time evolution of the macroscopic theoretical law $[\xi/(-\ln(1-\xi))]^{2\Delta}$ (dashed curves, eq. (4.12)) evaluated for $\Delta \in \{1, 3/2, 2\}$ with $\varepsilon = 0.1$ and $\beta = 2\pi$. The curves are normalized by their late-time saturation value, effectively setting the theoretical maximum to unity (dotted line). As $t \rightarrow \infty$ ($\xi \rightarrow 0$), the geometric spreading mathematically cancels the return amplitude decay, causing the raw negativity to strictly saturate to the constant plateau \mathcal{N}_∞ . This visualizes the asymptotic behavior described in Proposition 4.3 and demonstrates that the raw negativity is inherently bounded at late times, necessitating the seed-normalized diagnostic to probe continued infall.

Proposition 4.3 (Saturation of the raw negativity). *Within the macroscopic regime ($Q \gg 1$, $\langle \hat{N}_{\text{Krylov}} \rangle \ll D$) the raw Krylov–Wigner negativity approaches a constant plateau,*

$$\mathcal{N}_{\text{raw}}(t) \xrightarrow{t \rightarrow \infty} \mathcal{N}_\infty \equiv \frac{c_\Delta \Gamma(2\Delta)}{2^{\Delta-2} \Gamma(\Delta)} = \frac{2^{\Delta+1}}{\sqrt{\pi}} \Gamma\left(\Delta + \frac{1}{2}\right) c_\Delta, \quad c_\Delta = \int_0^\infty \frac{|J_\Delta(Z)|}{Z^\Delta} dZ, \quad (4.13)$$

a finite number that depends only on the conformal dimension Δ and is independent of the temperature β , the regulator ε , and the Hilbert-space dimension D . It is finite for every $\Delta > 1/2$ and decreases monotonically with Δ . The plateau is approached from below,

$$\mathcal{N}_{\text{raw}}(t) = \mathcal{N}_\infty \left(1 - \Delta \xi(t) + O(\xi^2)\right) = \mathcal{N}_\infty \left(1 - \Delta \frac{\varepsilon_0}{\sinh^2(\pi t/\beta)} + \dots\right), \quad (4.14)$$

i.e. exponentially on the thermal timescale, with relative deficit $\sim 4\Delta \varepsilon_0 e^{-2\pi t/\beta}$.

Proof. Setting $u \equiv -\ln(1 - \xi) = 2|\ln |A||$, equation (4.12) reads $\mathcal{N}_{\text{raw}} = \mathcal{N}_{\infty}(\xi/u)^{2\Delta}$. Since $u = \xi + \frac{1}{2}\xi^2 + O(\xi^3)$, $\xi/u = 1 - \frac{1}{2}\xi + O(\xi^2)$ and $(\xi/u)^{2\Delta} = 1 - \Delta\xi + O(\xi^2)$, which gives (4.14) on inserting $\xi \simeq \varepsilon_0/\sinh^2(\pi t/\beta)$; the limit $\xi \rightarrow 0$ yields (4.13). The second form of \mathcal{N}_{∞} follows from Legendre duplication. Convergence of c_{Δ} is controlled at the two ends: near $Z = 0$ the integrand tends to the constant $2^{-\Delta}/\Gamma(\Delta + 1)$, while at large Z , $|J_{\Delta}(Z)|/Z^{\Delta} \sim \sqrt{2/\pi} |\cos(\dots)| Z^{-\Delta-1/2}$, integrable precisely for $\Delta > 1/2$. \square

Why a spreading distribution has bounded negativity. The saturation is not an accident of the integral but a balance between two competing effects. As $|A| \rightarrow 1$ the mean Krylov level $\langle \hat{N}_{\text{Krylov}} \rangle = 2\Delta|A|^2/(1 - |A|^2) \simeq 2\Delta/\xi$ diverges, so the packet occupies an ever larger region of the chain; at the same time the peak height of W , set by the survival probability $\mathcal{P} = |\psi_0|^2 = \xi^{2\Delta}$, vanishes. In the negativity these effects are governed by the *same* power of ξ : the radial spread contributes $\int_0^{\infty} Q^{2\Delta-1} e^{-2Q|\ln |A||} dQ = \Gamma(2\Delta) (2|\ln |A||)^{-2\Delta} \propto \xi^{-2\Delta}$, which grows exactly as fast as the envelope $\mathcal{P} \propto \xi^{2\Delta}$ decays. The total absolute quasi-probability is their product, and the two powers cancel. Physically, the quasi-probability spreads to fill an ever larger region of phase space while thinning in height, holding the 1-norm of the signed distribution fixed once the state has delocalised, while the discrete-Wigner counterpart of a wavepacket whose non-classicality stops growing after it has spread over the phase space available to it.

Remark 4.4 (Diagnostic status and the meaning of the matching). Two points should be kept in mind, following Remark 3.3. (i) \mathcal{N} is the raw negativity divided by the survival probability; it is a rescaled diagnostic, not the Wigner negativity of a normalised state. (ii) Comparing (4.8) with $1/\mathcal{P} = (1 - |A|^2)^{-2\Delta}$, the two share the same leading late-time scaling $\sinh^{4\Delta}$ and differ only at subleading order ($2|\ln |A|| = -\ln(1 - \xi) = \xi + \frac{1}{2}\xi^2 + \dots$ versus $1 - |A|^2 = \xi$). Thus the leading growth of \mathcal{N} coincides with that of the inverse survival probability, and the matching identified in section 5 is, at leading order, a statement about the survival-probability decay exponent 2Δ rather than about the magnitude of the magic. The magic content enters through the coefficient \mathcal{N}_{∞} of (4.13) and the subleading structure. We therefore present the matching as a structural relation between boundary two-point data, not as a dynamical coincidence of magic with tidal effects.

5 Matching and the Critical Dimension

We now compare the normalized negativity rate (4.11) with the growth rate of the Krylov wavepacket variance. Both are functions of the single scaling variable $\xi(t)$ of (4.9), so the comparison reduces to matching two power laws.

Exact variance rate. From Lemma 3.1, $\text{Var}(\hat{N}_{\text{Krylov}}) = 2\Delta(1 - \xi)/\xi^2$, whose exact time derivative is, with $C \equiv \cosh(\pi t/\beta)$,

$$\boxed{\frac{d}{dt} \text{Var}(\hat{N}_{\text{Krylov}}) = \frac{4\Delta\pi}{\beta} \cdot \frac{\sinh(\pi t/\beta) \cosh(\pi t/\beta) [2 \sinh^2(\pi t/\beta) + \varepsilon_0]}{\varepsilon_0^2}}. \quad (5.1)$$

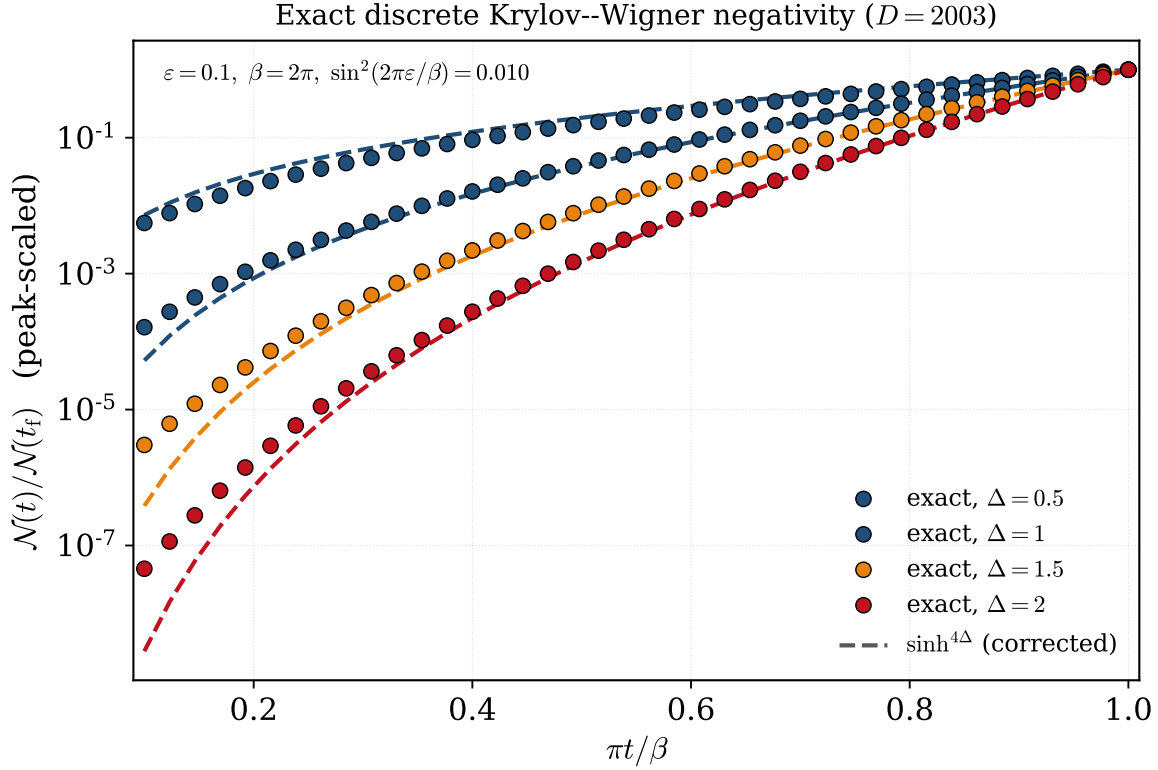


Figure 2. Growth of the seed-normalized negativity (log–log). The exact discrete seed-normalized negativity $\mathcal{N} = \mathcal{N}_{\text{raw}}/\mathcal{P}$ (markers), computed from the Wootters discrete Wigner function on the $\mathbb{Z}_D \times \mathbb{Z}_D$ phase space of prime dimension $D = 2003$ ($\varepsilon = 0.1, \beta = 2\pi$), plotted against $\sinh(\pi t/\beta)$ on log–log axes and divided by its value at $\pi t/\beta = 1$ (common footing). On these axes the continuum law $\mathcal{N} \sim \sinh^{4\Delta}$ (4.10) is a straight line of slope 4Δ (dashed); the exact markers follow it (fitted slopes 3.91, 5.79, 7.74 for $\Delta = 1, \frac{3}{2}, 2$ against 4, 6, 8), confirming that the seed-normalized negativity *grows* as a power law—in contrast to the raw negativity of figure 1, which saturates. The window is kept within the validity regime of the macroscopic description ($\langle \hat{N}_{\text{Krylov}} \rangle \ll D$, truncation weight $< 10^{-3}$). The marginal case $\Delta = \frac{1}{2}$ (open squares), where c_Δ diverges logarithmically, is shown for reference and carries a slow log-enhancement above the pure \sinh^2 slope.

This is exact for all $t > 0, \varepsilon > 0$. For $S^2 \gg \varepsilon_0$ the bracket reduces to $2S^2$, giving the late-time asymptotic

$$\frac{d}{dt} \text{Var}(\hat{N}_{\text{Krylov}}) \approx \frac{8\Delta\pi}{\beta} \frac{\sinh^3(\pi t/\beta) \cosh(\pi t/\beta)}{\sin^4(2\pi\varepsilon/\beta)}. \quad (5.2)$$

Matching through the single scaling variable. Both late-time rates (4.11) and (5.2) are powers of $\xi \simeq \varepsilon_0/S^2$, so their t - and ε -exponents are locked together:

Quantity	t -scaling	ε -scaling	Match condition
$\mathcal{R}(t)$	$\sinh^{4\Delta-1}(\pi t/\beta) \cosh(\pi t/\beta)$	$\sin^{-4\Delta}(2\pi\varepsilon/\beta)$	
$\frac{d \text{Var}}{dt}$	$\sinh^3(\pi t/\beta) \cosh(\pi t/\beta)$	$\sin^{-4}(2\pi\varepsilon/\beta)$	
<i>Equality requires</i>	$4\Delta - 1 = 3$	$4\Delta = 4$	$\Delta = 1$

Both rows give the same condition

$$4\Delta - 1 = 3 \implies \Delta = 1, \quad (5.3)$$

and they are not independent tests, since the t - and ε -exponents are tied together by ξ . At this value the two rates share the functional form $\sinh^3(\pi t/\beta) \cosh(\pi t/\beta) / \sin^4(2\pi\varepsilon/\beta)$, and we obtain the *late-time asymptotic* proportionality

$$\boxed{\mathcal{R}(t) \simeq \mathcal{A}(\beta, \varepsilon) \frac{d}{dt} \text{Var}(\hat{N}_{\text{Krylov}}), \quad \Delta = 1, \quad \sinh^2(\pi t/\beta) \gg \sin^2(2\pi\varepsilon/\beta),} \quad (5.4)$$

with $\mathcal{A}(\beta, \varepsilon)$ a t -independent constant. Away from $\Delta = 1$ the ratio $\mathcal{R}/(d \text{Var}/dt) \propto \sinh^{4\Delta-4}(\pi t/\beta)$ is not constant, so the proportionality holds if and only if $\Delta = 1$.

Remark 5.1 (Asymptotic, not exact). Relation (5.4) holds in the late-time regime $\sinh^2(\pi t/\beta) \gg \varepsilon_0$. The variance rate (5.1) is exact and retains the factor $2 \sinh^2(\pi t/\beta) + \varepsilon_0$, whereas the negativity rate comes from the macroscopic/Hankel form; the ratio reaches its constant plateau only once $\sinh^2 \gg \varepsilon_0$, and is not constant at finite time. No exact finite-time equality is claimed.

The critical dimension saturates the BF bound. The value $\Delta = 1$ is distinguished. Using $m^2 \ell_{\text{AdS}}^2 = \Delta(\Delta - 2)$ in AdS_3 ,

$$m^2 \ell_{\text{AdS}}^2|_{\Delta=1} = 1 \cdot (1 - 2) = -1, \quad (5.5)$$

which *saturates* the Breitenlohner–Freedman bound $m^2 \ell_{\text{AdS}}^2 \geq -1$ [45]. At this value the two roots $\Delta_{\pm} = 1 \pm \sqrt{1 + m^2 \ell_{\text{AdS}}^2}$ degenerate to $\Delta_+ = \Delta_- = 1$, the threshold of the stability window where the alternate (logarithmic) quantization applies. Unlike a generic light operator, the BF-saturating scalar sits exactly at the edge of stability—a distinguished, scheme-independent point. That the higher-moment (negativity) diagnostic singles out this edge, rather than the first-moment (complexity) diagnostic, is the structural observation of this work.

Figures 3–5 illustrate (5.4) using the exact formulas (3.5) and (5.1); with the corrected exponents the diagnostic ratio scales as $\sinh^{4\Delta-4}(\pi t/\beta)$ and is asymptotically flat only at $\Delta = 1$.

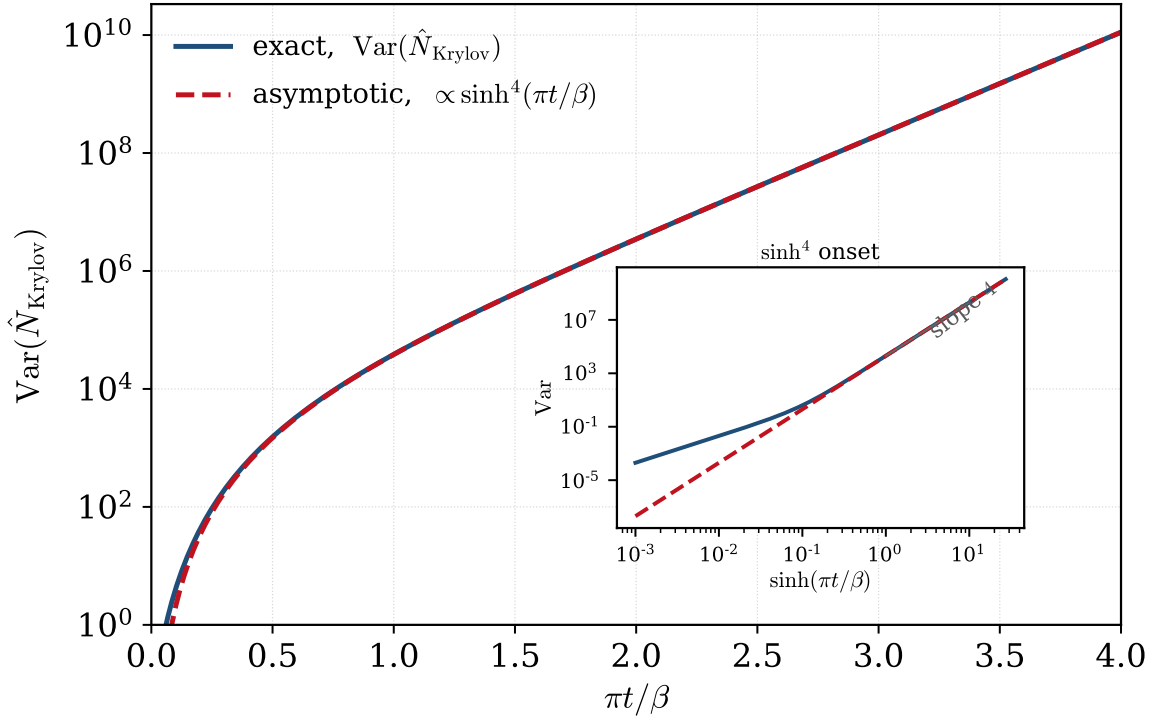


Figure 3. Exact growth of the Krylov wavepacket variance. $\text{Var}(\hat{N}_{\text{Krylov}})$ versus $\pi t/\beta$ from the negative-binomial formula (3.5) (solid) and its late-time \sinh^4 asymptotic (dashed), for $\sin^2(2\pi\varepsilon/\beta) = 0.01$ at $\Delta = 1$.

6 Negativity Rate as Tidal Momentum

The matching acquires a sharper bulk reading in the language of the holographic Krylov dictionary, in which the rate of spread complexity is a proper momentum. We show that the normalized negativity rate is governed by the *same* proper momentum, dressed by an explicit factor, and that this recasts the $\Delta = 1$ condition as the equality of two bulk momenta. The relations of this section rest on the exact boundary identity (3.6) and the dictionary (2.19); they do not invoke the operator identification of section 7.

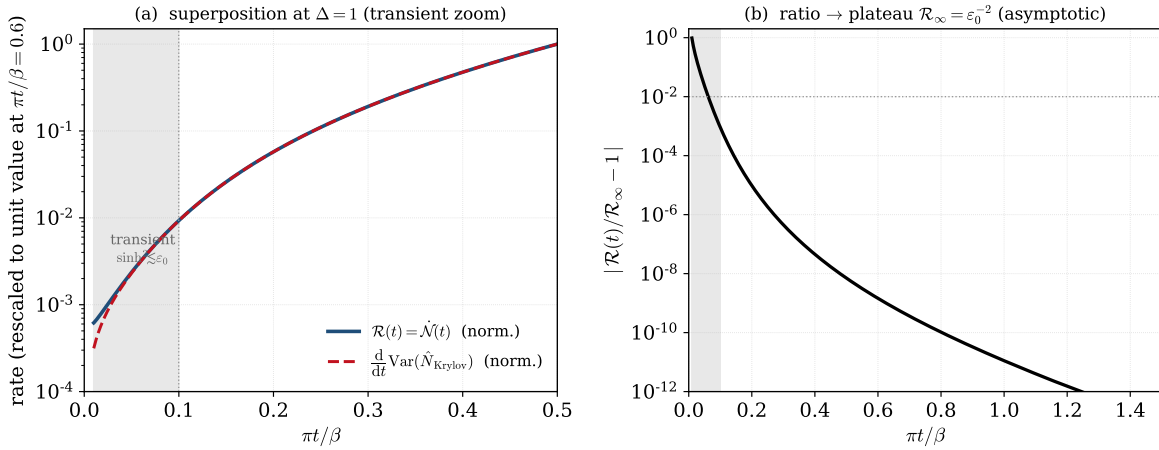
Recall the established first-moment entry [20]: with $\mathcal{C}(t) \equiv \langle \hat{N}_{\text{Krylov}} \rangle$,

$$\frac{d\mathcal{C}}{dt} \propto P_\rho(t), \quad (6.1)$$

and $\mathcal{C}(t) = \frac{2\Delta}{\varepsilon_0} \sinh^2(\pi t/\beta)$ exactly, so $P_\rho \propto \sinh(\pi t/\beta) \cosh(\pi t/\beta)$.

Variance rate (exact). The Krylov occupation is negative-binomial, so the variance is an exact quadratic function of the mean, $\text{Var} = \mathcal{C} + \mathcal{C}^2/2\Delta$ (3.6). Differentiating,

$$\frac{d\text{Var}(\hat{N}_{\text{Krylov}})}{dt} = \left(1 + \frac{\mathcal{C}}{\Delta}\right) \frac{d\mathcal{C}}{dt} \propto \left(1 + \frac{\mathcal{C}(t)}{\Delta}\right) P_\rho(t). \quad (6.2)$$



$\Delta = 1$, $\sin^2(2\pi\varepsilon/\beta) = 0.00996671$; onset scale $\pi t/\beta \sim \sqrt{\varepsilon_0}$. The two rates are distinct closed forms, coinciding as $\sinh^2(\pi t/\beta) \gg \varepsilon_0$.

Figure 4. Superposition of $\mathcal{R}(t)$ and $d\text{Var}/dt$ at $\Delta = 1$. (a) The normalized negativity rate $\mathcal{R} = \hat{\mathcal{N}}$ and the exact Krylov variance rate $\frac{d}{dt}\text{Var}(\hat{N}_{\text{Krylov}})$, each rescaled to unit value at the right edge, versus $\pi t/\beta$ (log scale), zoomed to the transient/onset region for $\sin^2(2\pi\varepsilon/\beta) = 0.01$. The grey band marks the transient $\sinh^2(\pi t/\beta) \lesssim \varepsilon_0$, i.e. $\pi t/\beta \lesssim \sqrt{\varepsilon_0}$, where the two rates differ; they coincide thereafter. The curves are built from *different* closed forms— \mathcal{R} from the macroscopic-exact negativity $\mathcal{N} \propto [\ln(1 + \varepsilon_0/\sinh^2(\pi t/\beta))]^{-2\Delta}$ and $\frac{d}{dt}\text{Var}$ from the exact rate (5.1)—so their agreement is not a tautology. (b) Relative deviation of the ratio $\mathcal{R}/\frac{d}{dt}\text{Var}$ from its late-time plateau $\mathcal{R}_\infty = \varepsilon_0^{-2}$ (log scale): it decreases monotonically to zero as $t \rightarrow \infty$, so the proportionality becomes exact in the asymptotic regime $\sinh^2(\pi t/\beta) \gg \varepsilon_0$ (Remark 5.1).

This is an *exact* boundary identity: the variance rate is the proper radial momentum dressed by the calculable factor $1 + \mathcal{C}/\Delta$.

Normalized negativity rate. From the corrected macroscopic result, $\mathcal{N} \propto \sinh^{4\Delta}(\pi t/\beta)$ (section 4.4), so $\mathcal{R} \propto \sinh^{4\Delta-1} \cosh$. Using $\mathcal{C} \propto \sinh^2$ and $P_\rho \propto \sinh \cosh$,

$$\mathcal{R}(t) \propto \sinh^{4\Delta-2} \cdot (\sinh \cosh) \propto \mathcal{C}(t)^{2\Delta-1} P_\rho(t). \quad (6.3)$$

Thus the negativity rate is the proper momentum dressed by $\mathcal{C}^{2\Delta-1}$, whereas the variance rate (6.2) is dressed by $1 + \mathcal{C}/\Delta \rightarrow \mathcal{C}/\Delta$ at late times. The two dressings coincide precisely when $2\Delta - 1 = 1$, i.e. $\Delta = 1$, reproducing (5.3) from the bulk-momentum side. At that dimension,

$$\boxed{\mathcal{R}(t) \propto \mathcal{C}(t) P_\rho(t) \quad (\Delta = 1)}, \quad (6.4)$$

the negativity rate is the product of the proper radial position (encoded in \mathcal{C}) and the proper radial momentum.

Geometric interpretation: geodesic deviation. The structure of (6.4) suggests the bulk observable dual to the negativity rate. The variance is the squared radial spread, $\text{Var} \leftrightarrow (\delta\rho)^2$,

$$\sin^2(2\pi\varepsilon/\beta) = 0.00996671$$

$$\text{ratio} \propto \sinh^{4\Delta-4}(\pi t/\beta)$$

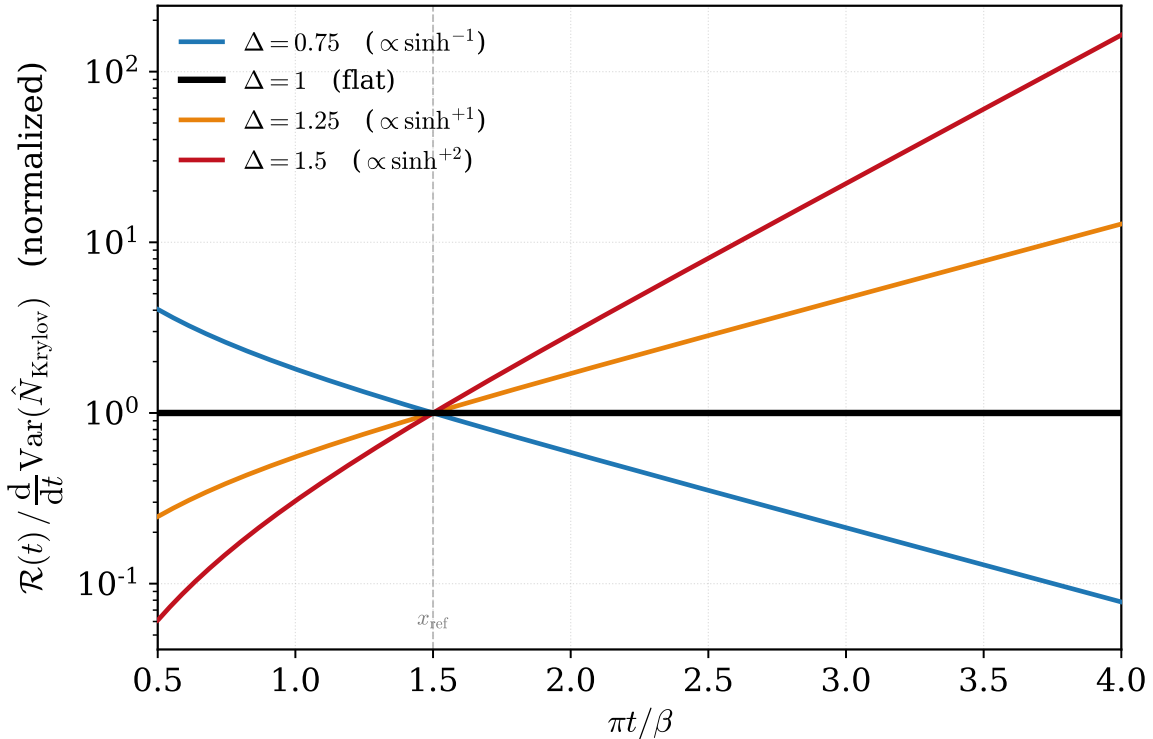


Figure 5. Diagnostic of the matching condition, with the asymptotics shown explicitly.

The ratio $\mathcal{R}(t)/\frac{d}{dt}\text{Var}(\hat{N}_{\text{Krylov}})$ for several Δ at $\sin^2(2\pi\varepsilon/\beta) = 0.01$, each normalized to unity at $x_{\text{ref}} \equiv \pi t/\beta = 1.5$ (so that every Δ -dependent prefactor, including c_Δ and the $O(1)$ lattice-convention factor, cancels; the plot is convention-independent). (a) The exact ratio (solid), built from the macroscopic-exact negativity $\mathcal{N} \propto [\ln(1 + \varepsilon_0/\sinh^2(\pi t/\beta))]^{-2\Delta}$ and the exact variance rate (5.1), peels away from its late-time asymptote $(\sinh(\pi t/\beta)/\sinh x_{\text{ref}})^{4\Delta-4}$ (dashed) at early times and merges onto it at late times. (b) The local logarithmic slope $d \ln \mathcal{R}/d \ln \sinh(\pi t/\beta)$ converges to the constant $4\Delta - 4$ (dotted guides). The ratio is thus flat *only* at the Breitenlohner–Freedman-saturating value $\Delta = 1$, decaying for $\Delta < 1$ and diverging for $\Delta > 1$; the flatness is an asymptotic statement, consistent with Remark 5.1.

whose rate is $\frac{d}{dt}(\delta\rho)^2 = 2\delta\rho(\dot{\delta\rho})$. The separation $\delta\rho$ between neighbouring infalling geodesics obeys the geodesic-deviation equation

$$\frac{D^2 \delta\rho}{d\tau^2} = -R^\rho{}_{\tau\tau\rho} \delta\rho, \quad (6.5)$$

so the relative (tidal) momentum $(\dot{\delta\rho})$ grows in proportion to the separation times the infall rate, and $\delta\rho(\dot{\delta\rho}) \propto \mathcal{C} P_\rho$ is the rate of tidal stretching. The complexity rate measures the classical

geodesic momentum, while the normalized negativity rate measures the tidal momentum of geodesic deviation—the quantum spreading about the classical trajectory. This reading is expressed through the proper-momentum dictionary alone and is independent of the operator identification, subject to the caveat of Remark 4.4 on the diagnostic nature of \mathcal{N} .

7 Discussion

We have presented a boundary calculation—the seed-normalized Krylov–Wigner distribution, its total negativity, and the negativity rate—and its interpretation as a second-moment companion to spread complexity. We summarise the established results, then develop, as a direction for future work, a speculative bulk string interpretation that retains all of the derivations while separating them cleanly from the boundary analysis.

7.1 Summary of Boundary Results

Seed-normalized calculus. By fixing the normalization at the level of the amplitudes—dividing out the return amplitude to form $\chi_n = \psi_n/\psi_0$ and the seed-normalized distribution $\mathcal{W} = W/\mathcal{P}$ (section 3)—the physically informative object is primary from the start. Its closed Bessel form (3.21) follows from the $SU(1, 1)$ coherent-state structure, Stirling asymptotics, and the Euler–Maclaurin formula, and carries no survival factor.

Negativity and its meaning. Evaluating the total negativity directly from the Bessel form, and keeping the Bessel variable $Z = Q\tilde{\theta}$ throughout, the radial power is $Q^{2\Delta-1}$ and the normalized negativity grows as $\mathcal{N}(t) \sim \sinh^{4\Delta}(\pi t/\beta)$ (4.10); the raw, normalised-state negativity instead saturates (4.12), consistent with $\mathcal{N}_{\text{raw}} \leq \sqrt{D}$ and the plateau of [23]. As stressed in Remarks 3.3 and 4.4, \mathcal{N} is a rescaled (survival-normalized) diagnostic whose leading growth coincides with the inverse survival probability; the matching is correspondingly a statement about the boundary two-point data. Proposition 4.2 (the rate, including the descendant-weight term) and the exact variance rate (5.1) are exact boundary results.

Matching and tidal momentum. The normalized negativity rate tracks the Krylov variance rate in the late-time asymptotic regime if and only if $\Delta = 1$ (5.4), a necessary, leading-order, asymptotic condition (Remark 5.1). The selected dimension *saturates* the Breitenlohner–Freedman bound ($m^2\ell_{\text{AdS}}^2 = -1$), the edge of the stability window. In the proper-momentum language of Caputa et al. [20] the rate is $\mathcal{R} \propto \mathcal{C}^{2\Delta-1}P_\rho$, coinciding with the variance dressing $(1 + \mathcal{C}/\Delta)P_\rho$ at $\Delta = 1$, where $\mathcal{R} \propto \mathcal{C}P_\rho$ is the rate of tidal stretching of neighbouring infalling geodesics (section 6).

7.2 Outlook

Several boundary questions remain. (i) The operational status of the seed-normalized negativity \mathcal{N} deserves sharpening—whether the physically preferred observable is the raw (bounded, saturating) negativity, the survival-normalized \mathcal{N} , or a differently conditioned quantity—since this fixes the physical content of the matching. (ii) The proportionality constant $\mathcal{A}(\beta, \varepsilon)$ in (5.4) should be determined by a microstate-level analysis. (iii) The same phase-space calculus

can be brought to bear on the stabilizer complexity of Hawking radiation [47–49], the Krylov complexity of purification for thermal states [50], and on toy models such as DSSYK, where the Krylov basis coincides with the chord-length basis [23, 37, 38]. The extended-probe regime has been examined concurrently in [46], which treats the extended case conservatively—as a controlled proposal rather than a first-principles derivation—consistent with the conjectural status we assign the operator identification.

7.3 Future Direction: A Bulk String Interpretation

This subsection is speculative and logically independent of the boundary results above. Its central object, the operator identification $\hat{N}_{\text{str}} \simeq \hat{N}_{\text{Krylov}}$, is a conjecture supported only by a shared Casimir (a necessary, not sufficient, condition); the tidal-activation mechanism is a heuristic. We include the full derivations here, as a program for future work, rather than in the main text.

A point particle cannot furnish a bulk avatar of the negativity: its Wigner function is Gaussian (positive), and Gaussian evolution preserves positivity, generating no negativity. Any bulk interpretation must involve genuine quantum internal degrees of freedom. We explore the possibility that the infalling excitation is a quantized fundamental string.

(i) Exactness of the WZW description. String propagation in AdS_3 is governed by the $\text{SL}(2, \mathbb{R})$ Wess–Zumino–Witten (WZW) model at level k , exactly solvable for $\text{AdS}_3 \times S^3 \times \mathcal{M}_4$ [40, 41]. The physical spectrum is organized by the discrete-series UIRs D_j^+ of $\text{SL}(2, \mathbb{R})$, with $m^2 \ell_{\text{AdS}}^2 = j(j-2)$ and $j = \Delta$. We use only the zero-mode (spacetime) $\mathfrak{su}(1, 1)$ Casimir of this sector.

(ii) The algebraic bridge. The Lanczos coefficients (2.7), from the CFT thermal two-point function, realize D_Δ^+ with Bargmann index $k = \Delta$ (Lemma 2.1); the string zero-mode algebra, via $j = \Delta$, realizes the *same* D_Δ^+ (Lemma 7.2). The discrete-series UIR is labelled by its Bargmann index, so the two carry the same representation—a necessary condition for identifying them, whose sufficiency is the content of Conjecture 7.4.

(iii) A heuristic activation mechanism (frame caveat). It is sometimes argued that higher transverse modes are populated because the local temperature $T_\beta/\sqrt{-g_{tt}}$ diverges near the horizon. This must be treated with care: $T_\beta/\sqrt{-g_{tt}}$ is the (Tolman) temperature registered by *static* observers, and diverges at the horizon for that reason. A freely-falling observer crossing the *regular* BTZ horizon sees no divergence—by the equivalence principle—and since BTZ is locally AdS_3 , the curvature invariants stay finite in the infalling Fermi frame (the tidal tensor is the constant $\Omega_\perp^2 \sim \ell_{\text{AdS}}^{-2}$ of Appendix D). A genuine near-horizon mechanism must therefore be argued from the global/thermal (quotient) structure of BTZ, not from a local curvature or temperature divergence. We retain the Hagedorn picture only as qualitative motivation.

Polyakov quantization and the string-size operator

We model the infalling excitation as a fundamental closed string. Gauge-fixing the Polyakov action to conformal gauge and then transverse light-cone gauge, and working in a Fermi normal frame anchored to the classical centre-of-mass geodesic (locally flat target metric), the transverse coordinates are free massless fields with the closed-string mode expansion

$$X^i(\tau, \sigma) = x^i + \alpha' p^i \tau + i\sqrt{\frac{\alpha'}{2}} \sum_{m \neq 0} \frac{1}{m} \left(\alpha_m^i e^{-im(\tau-\sigma)} + \tilde{\alpha}_m^i e^{-im(\tau+\sigma)} \right), \quad (7.1)$$

with $[\alpha_m^i, \alpha_n^j] = m\delta_{m+n,0}\delta^{ij}$ and similarly for $\tilde{\alpha}$. Squaring the transverse fluctuation δX^i and averaging over the worldsheet with $\frac{1}{2\pi} \int_0^{2\pi} e^{i(m+n)\sigma} d\sigma = \delta_{m+n,0}$ sets $n = -m$, producing *two* powers of $1/m$; the normally ordered, worldsheet-averaged square is therefore

$$\langle \Delta X^2 \rangle_{\text{str}} = \alpha' \sum_{m=1}^{\infty} \frac{1}{m^2} \langle \alpha_{-m}^i \alpha_m^i + \tilde{\alpha}_{-m}^i \tilde{\alpha}_m^i \rangle = \alpha' \sum_{m=1}^{\infty} \frac{1}{m} \langle \hat{n}_m^i + \tilde{\hat{n}}_m^i \rangle, \quad (7.2)$$

where $\alpha_{-m}^i \alpha_m^i = m \hat{n}_m^i$ with \hat{n}_m^i the occupation-number operator (from $[\alpha_m^i, \alpha_{-m}^i] = m$). The $1/m$ weighting in occupation-number language is the standard signature of near-horizon string spreading [22]: the m -th mode carries spatial extent $\sim \ell_s/m$. We define the *string-size operator*

$$\hat{N}_{\text{str}} \equiv \sum_{m=1}^{\infty} \frac{1}{m^2} (\alpha_{-m}^i \alpha_m^i + \tilde{\alpha}_{-m}^i \tilde{\alpha}_m^i) = \sum_{m=1}^{\infty} \frac{1}{m} (\hat{n}_m^i + \tilde{\hat{n}}_m^i), \quad (7.3)$$

so that $\widehat{\Delta X^2} = \ell_s^2 \hat{N}_{\text{str}}$ with $\alpha' = \ell_s^2$. This $1/m^2$ (equivalently $1/m$ in occupation number) weighting distinguishes \hat{N}_{str} from the raw mode-bilinear sum and from the level-number operator $N_{\text{level}} = \sum_m m \alpha_{-m}^i \alpha_m^i$.

Remark 7.1 (Spectral caveat). The eigenvalues of \hat{N}_{str} are $\sum_m \frac{1}{m} (n_m + \tilde{n}_m)$ with $n_m, \tilde{n}_m \in \mathbb{Z}_{\geq 0}$ —rational combinations—whereas \hat{N}_{Krylov} has the integer spectrum $\{0, 1, 2, \dots\}$. The identification can hold at most after a nontrivial reorganization of the transverse Fock space into the lowest-weight D_{Δ}^+ ladder; the shared Casimir does not by itself supply that reorganization.

Representation-theoretic structure and the conjecture

Lemma 7.2 (Casimir compatibility). *The discrete-series sector of the string Hilbert space \mathcal{H}_{str} relevant to the infalling dynamics carries a representation of $\mathfrak{su}(1, 1)$ whose quadratic Casimir equals $\Delta(\Delta - 1)$, coinciding with $C_2^{(K)} = \Delta(\Delta - 1)$ of the Krylov chain (Lemma 2.1).*

Proof. The $\text{SL}(2, \mathbb{R})$ WZW spectrum [40] is organized by the zero-mode $\mathfrak{sl}(2, \mathbb{R})$ with Casimir $j(j - 1)$ on a spin- j discrete-series state; the dictionary [43, 44] sets $j = \Delta$, giving $\Delta(\Delta - 1)$, matching (2.12). \square

Proposition 7.3 (Conditional operator identification). *Suppose \hat{N}_{str} of (7.3), restricted to the infalling discrete-series sector, is the lowest-weight number operator of that sector (its eigenstates of eigenvalue $n = 0, 1, 2, \dots$ form a lowest-weight ladder under an $\mathfrak{su}(1, 1)$ action*

with Bargmann index $k = \Delta$, with $\hat{N}_{\text{str}} = K_0^{(\text{str})} - \Delta$). Then there is a unitary $U : \mathcal{H}_{\text{str}} \rightarrow \mathcal{H}_{\text{Krylov}}$ with $UK_\mu^{(\text{str})}U^\dagger = K_\mu^{(K)}$ under which $\hat{N}_{\text{str}} = U^\dagger \hat{N}_{\text{Krylov}} U$, i.e. $\hat{N}_{\text{str}} \simeq \hat{N}_{\text{Krylov}}$, and all moments agree.

Proof. By Lemma 2.1 the Krylov chain realizes D_Δ^+ with $\hat{N}_{\text{Krylov}} = \text{diag}(0, 1, 2, \dots)$. Under the hypothesis \hat{N}_{str} acts likewise in the lowest-weight basis. UIRs of $\text{SU}(1, 1)$ with equal Bargmann index are unitarily equivalent [39]; mapping lowest-weight vector to lowest-weight vector fixes U up to a phase and yields the intertwining relations. \square

Conjecture 7.4 (Operator identification). *The hypothesis of Proposition 7.3 holds: \hat{N}_{str} , restricted to the infalling discrete-series sector, is unitarily equivalent to the lowest-weight number operator of D_Δ^+ , so that $\hat{N}_{\text{str}} \simeq \hat{N}_{\text{Krylov}}$.*

Remark 7.5 (Status). The shared Casimir is necessary but not sufficient. It guarantees an intertwiner between the abstract representations, but not that the physically defined \hat{N}_{str} —built from worldsheet oscillators, with the rational spectrum of Remark 7.1—is the lowest-weight Cartan generator rather than some other self-adjoint operator carrying the same representation. The spacetime $\text{SL}(2, \mathbb{R})$ organizing the WZW spectrum acts on zero-mode data, whereas \hat{N}_{str} measures transverse oscillator content; establishing the conjecture requires the explicit bulk-to-boundary map at finite string coupling and remains open.

The holographic variance map

Under Conjecture 7.4, all moments of \hat{N}_{str} and \hat{N}_{Krylov} agree. The mean maps the transverse spread to spread complexity, $\langle \Delta X^2 \rangle_{\text{str}} = \ell_s^2 \mathcal{C}$. The normalized negativity rate tracks the variance; mapping $\text{Var}(\widehat{\Delta X^2}) = \ell_s^4 \text{Var}(\hat{N}_{\text{Krylov}})$ and using the exact NB identity (3.6),

$$\boxed{\ell_s^2 \text{Var}(\hat{N}_{\text{Krylov}}) = \langle \Delta X^2 \rangle_{\text{str}} + \frac{1}{2\Delta\ell_s^2} \langle \Delta X^2 \rangle_{\text{str}}^2}, \quad (7.4)$$

exact within the negative-binomial structure and valid whenever Conjecture 7.4 holds. In the late-time limit $\langle \Delta X^2 \rangle_{\text{str}} \gg \ell_s^2$ the map is purely quadratic: the Krylov variance is driven by the *square* of the mean transverse spreading. Combined with the boundary matching, this would give—at $\Delta = 1$ and under the conjecture—the bulk reading

$$\mathcal{R}(t) \propto \frac{1}{\ell_s^4} \frac{d}{dt} \text{Var}(\widehat{\Delta X^2}) \simeq \frac{1}{2\Delta\ell_s^4} \frac{d}{dt} (\langle \Delta X^2 \rangle_{\text{str}}^2), \quad (7.5)$$

i.e. the normalized negativity rate as the rate of growth of the squared transverse string area. Making (7.5) precise—settling Conjecture 7.4, resolving the spectral mismatch of Remark 7.1, and re-examining the activation mechanism in the infalling frame—is left for future work.

Acknowledgments

I am deeply grateful to Prof. Onkar Parrikar for his mentorship, comprehensive assistance, and support throughout this project. I want to thank Prof. Saskia Demulder and my friend Dr. Rathindranath for a careful and extensive review of an earlier draft, whose detailed comments—on the phase-space negativity integral, the interpretation of the normalized diagnostic, the asymptotic status of the matching, the near-horizon frame, and the transverse-mode weighting—substantially improved both the derivations and their presentation. I also thank Avijit Sinha, Pruthvi Suriyadevara, and Jyotirmoy Mukherjee for helpful discussions, and acknowledge the support of the Department of Theoretical Physics, TIFR, Mumbai. Further comments and corrections on this draft are welcome.

A Stirling Asymptotics and the Gamma Kernel

The continuum limit rests on the large- Q behaviour of the kernel in (3.18),

$$K(Q, m) = \frac{\sqrt{\Gamma(2\Delta + Q + m)\Gamma(2\Delta + Q - m)}}{\sqrt{(Q + m)!(Q - m)!}}. \quad (\text{A.1})$$

Writing $(Q \pm m)! = \Gamma(Q \pm m + 1)$, the square factorises into two ratios of identical structure,

$$K(Q, m)^2 = \frac{\Gamma(2\Delta + Q + m)}{\Gamma(Q + m + 1)} \cdot \frac{\Gamma(2\Delta + Q - m)}{\Gamma(Q - m + 1)}. \quad (\text{A.2})$$

Each factor is $\Gamma(z + a)/\Gamma(z + b)$ with $z = Q \pm m$, $a = 2\Delta$, $b = 1$. Stirling's expansion $\ln \Gamma(z) = (z - \frac{1}{2}) \ln z - z + \frac{1}{2} \ln(2\pi) + O(z^{-1})$ gives

$$\frac{\Gamma(z + a)}{\Gamma(z + b)} = z^{a-b} \left[1 + \frac{(a-b)(a+b-1)}{2z} + O(z^{-2}) \right], \quad (\text{A.3})$$

so with $a - b = 2\Delta - 1$,

$$K(Q, m)^2 = (Q + m)^{2\Delta-1} (Q - m)^{2\Delta-1} \left[1 + \Delta(2\Delta - 1) \left(\frac{1}{Q+m} + \frac{1}{Q-m} \right) + \dots \right], \quad (\text{A.4})$$

and taking the positive square root and passing to $x = m/Q \in [-1, 1]$,

$$\boxed{K(Q, x) \simeq Q^{2\Delta-1} (1 - x^2)^{\Delta-1/2}}. \quad (\text{A.5})$$

The relative correction is uniformly $O(1/Q)$ for x bounded away from ± 1 . Near $x = \pm 1$ Stirling degrades, but the weight $(1 - x^2)^{\Delta-1/2}$ vanishes there for every $\Delta > 1/2$, so the boundary region carries negligible measure—the same vanishing that removes the Euler–Maclaurin boundary terms in Appendix B.

B Euler–Maclaurin Continuum Limit

With Appendix A, the mode sum in (3.18) becomes

$$\sum_{m=-Q}^Q f(m), \quad f(m) = K(Q, m) e^{im\theta} \simeq Q^{2\Delta-1} \left(1 - \frac{m^2}{Q^2}\right)^{\Delta-1/2} e^{iZm/Q}, \quad (\text{B.1})$$

with $\theta \equiv 4\pi p/D + 2\varphi_A$ and $Z \equiv Q\theta$. The Euler–Maclaurin formula

$$\sum_{m=-Q}^Q f(m) = \int_{-Q}^Q f \, dm + \frac{f(Q) + f(-Q)}{2} + \sum_{k \geq 1} \frac{B_{2k}}{(2k)!} \left[f^{(2k-1)}(Q) - f^{(2k-1)}(-Q) \right] + R \quad (\text{B.2})$$

has only boundary corrections. Changing variables $x = m/Q$,

$$\sum_{m=-Q}^Q f(m) \approx Q^{2\Delta} \int_{-1}^1 (1-x^2)^{\Delta-1/2} e^{iZx} \, dx. \quad (\text{B.3})$$

For $\Delta > 1/2$ the weight has an algebraic zero at $x = \pm 1$, so $f(\pm Q) = 0$; the residual sum–integral mismatch is suppressed by a positive power of Q (in the boundary layer $m = Q - s$, $f \simeq 2^{\Delta-1/2} Q^{\Delta-1/2} s^{\Delta-1/2} e^{iZm/Q}$, of order $Q^{\Delta-1/2}$ against the leading $Q^{2\Delta}$, giving a relative $O(Q^{-(\Delta+1/2)})$; the smooth interior contributes $O(Q^{-2})$). The integral (B.3) is Poisson’s Bessel representation (3.20); reinstating the prefactor $|A|^{2Q}/(D \Gamma(2\Delta))$ and collapsing via Legendre duplication $\Gamma(2\Delta) = 2^{2\Delta-1} \pi^{-1/2} \Gamma(\Delta) \Gamma(\Delta + \frac{1}{2})$,

$$\frac{1}{\Gamma(2\Delta)} \cdot \sqrt{\pi} \Gamma\left(\Delta + \frac{1}{2}\right) \cdot 2^\Delta = \frac{\pi}{2^{\Delta-1} \Gamma(\Delta)}, \quad (\text{B.4})$$

reproduces the closed-form distribution (3.21).

C Direct Evaluation of the Normalized Negativity

This appendix records the evaluation of the seed-normalized negativity $\mathcal{N}(t)$ from the macroscopic Bessel envelope (3.21), *keeping the Bessel variable $Z = Q\tilde{\theta}$ throughout*. The essential point is that the change of variables from the angular coordinate $\tilde{\theta}$ to Z carries an explicit factor $1/Q$.

Continuum limit. With $\tilde{\theta} = 4\pi p/D + 2\varphi_A$ and $\sum_p \rightarrow \frac{D}{4\pi} \int d\tilde{\theta}$,

$$\mathcal{N}(t) \approx \frac{D}{4\pi} \int_0^\infty dQ \int d\tilde{\theta} |\mathcal{W}(Q, \tilde{\theta}, t)|, \quad |\mathcal{W}| = \frac{\pi Q^{2\Delta}}{D 2^{\Delta-1} \Gamma(\Delta)} e^{-2Q|\ln|A||} \frac{|J_\Delta(Z)|}{Z^\Delta}. \quad (\text{C.1})$$

Note the absence of any survival factor $\mathcal{P} = |\psi_0|^2$: it was divided out at the level of the amplitudes (3.14).

Angular integral (the corrected step). Substituting $Z = Q\tilde{\theta}$, $d\tilde{\theta} = dZ/Q$,

$$\int d\tilde{\theta} \frac{|J_\Delta(Z)|}{Z^\Delta} = \frac{1}{Q} \int_0^\infty dZ \frac{|J_\Delta(Z)|}{Z^\Delta} = \frac{c_\Delta}{Q}, \quad c_\Delta = \int_0^\infty \frac{|J_\Delta(Z)|}{Z^\Delta} dZ. \quad (\text{C.2})$$

The integral c_Δ is finite for $\Delta > 1/2$: the integrand is regular at $Z = 0$ ($\rightarrow 2^{-\Delta}/\Gamma(\Delta + 1)$) and decays as $Z^{-\Delta-1/2}$ at large Z . The naive large- Z (Hankel) form alone would make the $\tilde{\theta}$ -integral diverge at $\tilde{\theta} \rightarrow 0$; that “divergence” is the region $Z \lesssim 1$ where the Hankel form fails, whose proper treatment is precisely the finite c_Δ together with the factor $1/Q$.

Radial integral and assembly. The $1/Q$ reduces the radial power to $Q^{2\Delta-1}$:

$$\int_0^\infty dQ Q^{2\Delta-1} e^{-2Q|\ln|A||} = \frac{\Gamma(2\Delta)}{(2|\ln|A||)^{2\Delta}}, \quad (\text{C.3})$$

so that

$$\boxed{\mathcal{N}(t) \approx \frac{c_\Delta \Gamma(2\Delta)}{2^{\Delta+1} \Gamma(\Delta)} \frac{1}{(2|\ln|A(t)||)^{2\Delta}}}, \quad (\text{C.4})$$

which is (4.8). Since $2|\ln|A|| = -\ln(1-\xi) \simeq \xi \simeq \varepsilon_0/S^2$ at late times, $\mathcal{N}(t) \simeq \text{const} \cdot \sinh^{4\Delta}(\pi t/\beta)/\sin^{4\Delta}(2\pi\varepsilon/\beta)$, the growth used in section 4.4. The raw negativity is recovered as $\mathcal{N}_{\text{raw}} = \mathcal{P}\mathcal{N} = (c_\Delta \Gamma(2\Delta)/2^{\Delta+1} \Gamma(\Delta)) [\xi/(-\ln(1-\xi))]^{2\Delta}$, which tends to the constant $c_\Delta \Gamma(2\Delta)/2^{\Delta+1} \Gamma(\Delta)$ as $\xi \rightarrow 0$: the normalised-state negativity saturates.

D A Dynamical Heuristic for the Operator Identification

We record a dynamical heuristic for Conjecture 7.4 that engages the worldsheet operator \hat{N}_{str} of (7.3) directly. *As with the future-direction discussion of section 7.3, this is motivational, not a proof; the frame caveat of section 7.3(iii) applies throughout.*

Transverse fluctuations and geodesic deviation

Writing the worldsheet field as a centre-of-mass geodesic $x^\mu(\tau)$ plus a transverse fluctuation δX^i , the geodesic-deviation expansion of the Polyakov equations gives

$$(\partial_\tau^2 - \partial_\sigma^2) \delta X^i + \mathcal{A}^i_j(\tau) \delta X^j = 0, \quad \mathcal{A}^i_j(\tau) \equiv R^i_{\mu j \nu} \dot{x}^\mu \dot{x}^\nu, \quad (\text{D.1})$$

with \mathcal{A}^i_j the tidal tensor [22, 42]. The curvature term supplies the transverse modes with a τ -dependent frequency.

The tidal frequency in AdS₃

Because AdS₃ is maximally symmetric, $R_{\mu\nu\rho\sigma} = -\ell_{\text{AdS}}^{-2} (g_{\mu\rho}g_{\nu\sigma} - g_{\mu\sigma}g_{\nu\rho})$, the transverse tidal tensor is $\mathcal{A}^i_j = \Omega_\perp^2 \delta_j^i$ with $\Omega_\perp^2 \sim \ell_{\text{AdS}}^{-2}$ a constant set by the curvature scale. We emphasise (cf. the frame caveat) that this local invariant does *not* diverge at the horizon; any enhancement of mode production must come from the relation to boundary time, $d\tau/dt = \sqrt{-g_{tt}}$, i.e. from the static-frame redshift rather than from local curvature. Each transverse mode obeys

$$\ddot{c}_m^i + \Omega_m^2(\tau) c_m^i = 0, \quad \Omega_m^2(\tau) = m^2 + \Omega_\perp^2(\tau). \quad (\text{D.2})$$

The squeezing $SU(1, 1)$ of the oscillators

A time-dependent frequency evolves the in-vacuum into a two-mode squeezed state via a Bogoliubov transformation $\alpha_m^i(t) = u_m \alpha_m^i + v_m \tilde{\alpha}_{-m}^{i\dagger}$, $|u_m|^2 - |v_m|^2 = 1$, whose generators are quadratic in the oscillators,

$$\kappa_+^{(m)} = \alpha_{-m}^i \tilde{\alpha}_{-m}^i, \quad \kappa_-^{(m)} = (\kappa_+^{(m)})^\dagger, \quad \kappa_0^{(m)} = \frac{1}{2}(\alpha_{-m}^i \alpha_m^i + \tilde{\alpha}_{-m}^i \tilde{\alpha}_m^i) + \text{const}, \quad (\text{D.3})$$

and close on $\mathfrak{su}(1, 1)$. The relevant $SU(1, 1)$ for \hat{N}_{str} is this squeezing algebra, acting on the transverse oscillator content, *not* the spacetime zero-mode algebra of Lemma 7.2—the distinction underlying Remark 7.5. The infalling transverse vacuum is, mode by mode, an $SU(1, 1)$ coherent state [39].

Negative-binomial occupation and the effective index

For a mode-pair with Bargmann index k_m and squeezing $\lambda_m = \tanh^2 r_m$, the occupation is

$$P_m(n) = \binom{n + 2k_m - 1}{n} (1 - \lambda_m)^{2k_m} \lambda_m^n, \quad (\text{D.4})$$

identical in form to (3.3). Under a common tidal drive the aggregate is again an $SU(1, 1)$ coherent state, with an effective index

$$k_{\text{eff}} = \sum'_{m \geq 1} \frac{k_m}{m^2}, \quad (\text{D.5})$$

where the $1/m^2$ weight is inherited from the corrected \hat{N}_{str} of (7.3) and the prime denotes a regularization of the mode sum. The aggregate occupation is $\text{NB}(2k_{\text{eff}}, |A|^2)$, coinciding with the Krylov distribution when

$$\boxed{k_{\text{eff}} = \Delta}, \quad (\text{D.6})$$

equivalently $k_{\text{eff}}(k_{\text{eff}} - 1) = \Delta(\Delta - 1)$, reproducing Lemma 7.2 from the worldsheet side.

Status

This heuristic shows that (i) the transverse oscillators acquire a curvature-induced τ -dependent frequency; (ii) their evolution is an $SU(1, 1)$ squeezing built from the oscillators \hat{N}_{str} counts; and (iii) the resulting occupation is negative-binomial. It does *not* constitute a proof: the matching (D.6) requires that the regularized sum (D.5) and the precise redshift profile conspire to give $k_{\text{eff}} = \Delta$; the identification of the aggregate number operator with \hat{N}_{Krylov} (rather than a level-dependent reshuffling with the same Casimir, cf. the rational spectrum of Remark 7.1) requires the explicit bulk-to-boundary map; and, per the frame caveat, the activation itself is not a local-curvature effect. We therefore retain the identification as a conjecture.

References

- [1] J. M. Maldacena, *The Large N limit of superconformal field theories and supergravity*, *Adv. Theor. Math. Phys.* **2** (1998) 231 [[hep-th/9711200](#)].
- [2] E. Witten, *Anti-de Sitter space and holography*, *Adv. Theor. Math. Phys.* **2** (1998) 253 [[hep-th/9802150](#)].
- [3] S. S. Gubser, I. R. Klebanov and A. M. Polyakov, *Gauge theory correlators from noncritical string theory*, *Phys. Lett. B* **428** (1998) 105 [[hep-th/9802109](#)].
- [4] L. Susskind, *Computational Complexity and Black Hole Horizons*, *Fortsch. Phys.* **64** (2016) 24 [[arXiv:1403.5695](#)].
- [5] D. Stanford and L. Susskind, *Complexity and Shock Wave Geometries*, *Phys. Rev. D* **90** (2014) 126007 [[arXiv:1406.2678](#)].
- [6] A. R. Brown, D. A. Roberts, L. Susskind, B. Swingle and Y. Zhao, *Holographic Complexity Equals Bulk Action?*, *Phys. Rev. Lett.* **116** (2016) 191301 [[arXiv:1509.07876](#)].
- [7] A. R. Brown, D. A. Roberts, L. Susskind, B. Swingle and Y. Zhao, *Complexity, action, and black holes*, *Phys. Rev. D* **93** (2016) 086006 [[arXiv:1512.04993](#)].
- [8] L. Susskind, *Three Lectures on Complexity and Black Holes*, *Springer* (2020) [[arXiv:1810.11563](#)].
- [9] V. Balasubramanian, J. M. Magan, P. Nandi and Q. Wu, *Spread complexity and the saturation of wormhole size*, [arXiv:2412.02038](#).
- [10] M. A. Nielsen, *A geometric approach to quantum circuit lower bounds*, [quant-ph/0502070](#).
- [11] R. Jefferson and R. C. Myers, *Circuit complexity in quantum field theory*, *JHEP* **10** (2017) 107 [[arXiv:1707.08570](#)].
- [12] P. Caputa, N. Kundu, M. Miyaji, T. Takayanagi and K. Watanabe, *Liouville Action as Path-Integral Complexity: From Continuous Tensor Networks to AdS/CFT*, *JHEP* **11** (2017) 097 [[arXiv:1706.07056](#)].
- [13] P. Caputa and J. M. Magan, *Quantum Computation as Gravity*, *Phys. Rev. Lett.* **122** (2019) 231302 [[arXiv:1807.04422](#)].
- [14] V. Balasubramanian, P. Caputa, J. M. Magan and Q. Wu, *Quantum complexity of time evolution with chaotic Hamiltonians*, *Phys. Rev. D* **106** (2022) 046007 [[arXiv:2202.06957](#)].
- [15] D. E. Parker, X. Cao, A. Avdoshkin, T. Schmitt and E. Altman, *A Universal Operator Growth Hypothesis*, *Phys. Rev. X* **9** (2019) 041017 [[arXiv:1812.08657](#)].
- [16] J. L. F. Barbón, E. Rabinovici, R. Shir and R. Sinha, *On The Evolution Of Operator Complexity Beyond Scrambling*, *JHEP* **10** (2019) 264 [[arXiv:1907.05393](#)].
- [17] V. Balasubramanian, M. Decross, A. Kar and O. Parrikar, *Quantum Complexity of Time Evolution with Chaotic Hamiltonians*, *JHEP* **01** (2020) 134 [[arXiv:1905.05765](#)].
- [18] P. Caputa, J. M. Magan and D. Patramanis, *Geometry of Krylov complexity*, *Phys. Rev. Res.* **4** (2022) 013041 [[arXiv:2109.03824](#)].
- [19] A. Bhattacharya, R. N. Das, B. Dey and J. Erdmenger, *Spread complexity and localization in PT -symmetric systems*, [[arXiv:2406.03524](#)].

- [20] P. Caputa, B. Chen, R. W. McDonald, J. Simón and B. Strittmatter, *Spread Complexity Rate as Proper Momentum*, [arXiv:2410.23334](#).
- [21] S. Banerjee, P. Basteiro, R. N. Das and M. Dorband, *Geometric quantum discord signals non-factorization*, *JHEP* **08** (2023) 104.
- [22] L. Susskind, *String theory and the principle of black hole complementarity*, *Phys. Rev. Lett.* **71** (1993) 2367 [[hep-th/9307168](#)].
- [23] R. Basu, A. Ganguly, S. Nath and O. Parrikar, *Complexity Growth and the Krylov–Wigner function*, *JHEP* **05** (2024) 264 [[arXiv:2402.13694](#)].
- [24] W. K. Wootters, *A Wigner-function formulation of finite-state quantum mechanics*, *Annals Phys.* **176** (1987) 1.
- [25] V. Veitch, C. Ferrie, D. Gross and J. Emerson, *Negative Quasi-Probability as a Resource for Quantum Computation*, *New J. Phys.* **14** (2012) 113011 [[arXiv:1201.1256](#)].
- [26] R. L. Hudson, *When is the Wigner quasi-probability density non-negative?*, *Rept. Math. Phys.* **6** (1974) 249.
- [27] R. Basu, P. Chowdhury, A. Ganguly, S. Nath, O. Parrikar and S. Paul, *Wigner negativity, random matrices and gravity*, *JHEP* **01** (2026) 106.
- [28] D. A. Roberts, D. Stanford and L. Susskind, *Localized shocks*, *JHEP* **03** (2015) 051 [[arXiv:1409.8180](#)].
- [29] P. Hosur, X.-L. Qi, D. A. Roberts and B. Yoshida, *Chaos in quantum channels*, *JHEP* **02** (2016) 004 [[arXiv:1511.04021](#)].
- [30] J. Maldacena, S. H. Shenker and D. Stanford, *A bound on chaos*, *JHEP* **08** (2016) 106 [[arXiv:1503.01409](#)].
- [31] V. S. Viswanath and G. Müller, *The Recursion Method: Application to Many-Body Dynamics* (Springer Berlin Heidelberg, 1994).
- [32] M. Banados, C. Teitelboim and J. Zanelli, *The Black hole in three-dimensional space-time*, *Phys. Rev. Lett.* **69** (1992) 1849 [[hep-th/9204099](#)].
- [33] P. Caputa, J. Simón, A. Stikonas and T. Takayanagi, *Quantum Entanglement of Localized Excited States at Finite Temperature*, *JHEP* **01** (2015) 102 [[arXiv:1410.2287](#)].
- [34] V. Malvimat, S. Porey and B. Roy, *Krylov Complexity in 2d CFTs with $SL(2, \mathbb{R})$ deformed Hamiltonians*, [arXiv:2402.15835](#).
- [35] P. Caputa, J. M. Magan, D. Patramanis and E. Tonni, *Krylov complexity in 2D CFTs*, *Phys. Rev. D* **109** (2024) 086004 [[arXiv:2306.14732](#)].
- [36] P. Caputa and S. Datta, *Operator growth in 2d CFT*, *JHEP* **12** (2021) 188 [[arXiv:2110.10519](#)].
- [37] V. Balasubramanian, J. M. Magan and Q. Wu, *Tridiagonalizing random matrices*, *Phys. Rev. D* **107** (2023) 126001 [[arXiv:2208.08452](#)].
- [38] V. Balasubramanian, J. M. Magan and Q. Wu, *Quantum chaos, integrability, and late times in the Krylov basis*, *Phys. Rev. E* **111** (2025) 014218 [[arXiv:2312.03848](#)].
- [39] A. Perelomov, *Generalized Coherent States and Their Applications* (Springer-Verlag, 1986).

- [40] J. M. Maldacena and H. Ooguri, *Strings in AdS₃ and the SL(2, ℝ) WZW model. Part 1: The spectrum*, *J. Math. Phys.* **42** (2001) 2929 [[hep-th/0005183](#)].
- [41] J. M. Maldacena and H. Ooguri, *Strings in AdS₃ and the SL(2, ℝ) WZW model. Part 2: Euclidean black hole*, *Phys. Rev. D* **65** (2002) 106006 [[hep-th/0111180](#)].
- [42] G. T. Horowitz and J. Polchinski, *Correspondence principle for black holes and strings*, *Phys. Rev. D* **55** (1997) 6189 [[hep-th/9612080](#)].
- [43] V. Balasubramanian, P. Kraus and A. E. Lawrence, *Bulk versus boundary dynamics in anti-de Sitter space-time*, *Phys. Rev. D* **59** (1999) 046003 [[hep-th/9805171](#)].
- [44] G. T. Horowitz and V. E. Hubeny, *Quasinormal modes of AdS black holes and the approach to thermal equilibrium*, *Phys. Rev. D* **62** (2000) 024027 [[hep-th/9909056](#)].
- [45] P. Breitenlohner and D. Z. Freedman, *Stability in Gauged Extended Supergravity*, *Annals Phys.* **144** (1982) 249.
- [46] A. Fatemiabhari, H. Nastase and D. Roychowdhury, *Holographic Krylov complexity in $\mathcal{N} = 4$ SYM theory*, *Phys. Rev. D* (2026) [[arXiv:2511.19286](#)].
- [47] R. Basu, O. Parrikar, S. Paul and H. Rajgadia, *On the stabilizer complexity of Hawking radiation*, [arXiv:2510.18967](#).
- [48] D. N. Page, *Information in black hole radiation*, *Phys. Rev. Lett.* **71** (1993) 3743 [[hep-th/9306083](#)].
- [49] G. Penington, *Entanglement Wedge Reconstruction and the Information Paradox*, *JHEP* **09** (2020) 002 [[arXiv:1905.08255](#)].
- [50] R. N. Das and T. Mori, *Krylov complexity of purification*, [[arXiv:2408.00826](#)].